NACA TN 2387

NATIONAL ADVISORY COMMITTEE
FOR AERONAUTICS

TECHNICAL NOTE 2387

THREE-DIMENSIONAL UNSTEADY LIFT PROBLEMS IN HIGH-SPEED

FLIGHT - THE TRIANGULAR WING

By Harvard Lomax, Max. A. Heaslet,
and Franklyn B. Fuller

Ames Aeronautical Laboratory
Moffett Field, Calif.

NACA

Washington
June 1951

NATIONAL ADVISORY COMMITTEE FOR AERONAUTICS

TECHNICAL NOTE 2387

THREE–DIMENSIONAL UNSTEADY LIFT PROBLEMS IN HIGH–SPEED

FLIGHT — THE TRIANGULAR WING

By Harvard Lomax, Max. A. Heaslet,
and Franklyn B. Fuller

SUMMARY

The indicial lift and pitching–moment coefficients are derived for flat–plate triangular wings traveling at supersonic speeds. The coefficients are determined for angle–of–attack distributions corresponding to sinking wings and to pitching wings. The wing with supersonic edges is completely analyzed, and the wing with subsonic edges is partially analyzed, the solution in this case being completed for very narrow wings by an application of slender wing theory. In the case of the supersonic edges, a comparison is made with known two–dimensional results and also with the results for the same triangular wing in reversed flow.

INTRODUCTION

The wing of triangular plan form has received considerable attention in the steady–state theory of three–dimensional wings in a supersonic stream. The purpose of the present report is to determine the aerodynamic characteristics of a triangular wing in supersonic unsteady motion.

There are several simple types of unsteady motion on which the analysis can be based. The so–called indicial motion, in which the velocity undergoes a discontinuous change at $t'=0$, will be considered here. (See also references 1 and 2.) It is possible to conceive the physical situation in two slightly different ways. For one, it can be supposed that the wing has been traveling at the constant velocity V_o for an infinitely long time and then, at $t'=0$, starts suddenly to sink without pitching motion (or to pitch without sinking) while maintaining the forward velocity V_o. On the other hand, the wing may be considered to be at rest in still air until at $t'=0$ it starts suddenly either to sink or to pitch and, at the same instant, attains the forward velocity V_o. The latter physical picture will be used in this report. Problems of unsteady motion can also be approached with the initial assumption that the velocity potential depends harmonically on the time. (See reference 3.) These two approaches are quite compatible in that they

can be related through the use of superposition methods (Duhamel's integral, Fourier's integral) of the operational calculus.

The question of whether the coordinate system should move with the wing or remain fixed is also of some importance. (See reference 4 for a discussion.) The latter alternative, that is, where the wing moves away from the coordinate system, was chosen for this report because the velocity potential φ in this case satisfies the wave equation

$$\varphi_{xx} + \varphi_{yy} + \varphi_{zz} - \frac{1}{a_0^2} \varphi_{t't'} = 0$$

where x, y, z are Cartesian coordinates, t' is time, and a_0 is the speed of sound in the undisturbed medium. The fact that the equation has this form is helpful in establishing analogs between steady and nonsteady motions, and these analogs are of considerable help in the solution of certain problems.

The boundary conditions to be considered correspond to the problem of the flat sinking wing (angle-of-attack distribution uniform over the plan form) and to the flat pitching wing (angle of attack varies linearly with chordwise distance) in indicial motion. First, the loading on a flat triangular wing with supersonic edges undergoing an indicial sinking motion is determined. Then a simplified method is developed whereby total lift and pitching-moment coefficient for the wing with supersonic edges may be obtained. These quantities are determined as functions of time, for both sinking and pitching wings.

Lastly, the triangular wing with subsonic edges is partially analyzed, and an approximate method for very slender wings is used to complete the determination of loading. The analog method, mentioned previously, is here of great value. Lift and pitching-moment coefficients for the sinking and pitching slender triangular wing are determined.

LIST OF IMPORTANT SYMBOLS

a_0 speed of sound in the free stream

c_0 root chord of triangular wing

C_L lift coefficient $\left(\dfrac{\text{lift}}{\frac{1}{2}\rho_0 V_0^2 S}\right)$

C_{L_α} indicial lift coefficient due to angle-of-attack change (without pitching) $\left(C_{L_\alpha} = \dfrac{\partial C_L}{\partial \alpha}\bigg|_{\alpha=0}\right)$

$C_{L_q}{}'$ indicial lift coefficient due to pitching on a wing rotating about its leading edge or apex $\left(C_{L_q} = \dfrac{\partial C_L}{\partial \dfrac{c_o \dot{\theta}}{V_o}}\bigg|_{\dot{\theta}=0} \right)$

C_m pitching-moment coefficient, positive when trailing edge tends to sink relative to leading edge

$C_{m_\alpha}{}'$ indicial pitching-moment coefficient due to angle-of-attack change (without pitching) measured about the leading edge or apex $\left(C_{m_\alpha}{}' = \dfrac{\partial C_m{}'}{\partial \alpha}\bigg|_{\alpha=0} \right)$

$C_{m_q}{}'$ indicial pitching-moment coefficient due to pitching measured about the leading edge or apex $\left(C_{m_q}{}' = \dfrac{\partial C_m{}'}{\partial \dfrac{c_o \theta}{V_o}}\bigg|_{\dot{\theta}=0} \right)$

m cotangent of sweep angle (cot Λ)

M_o free-stream Mach number $\left(\dfrac{V_o}{a_o} \right)$

P_o $\dfrac{M_o}{2\alpha s} \displaystyle\int_{-s}^{s} \dfrac{\Delta p}{q_o}\, dy$

P_1 $\dfrac{m M_o V_o}{2 \dot{\theta} s^2} \displaystyle\int_{-s}^{s} \dfrac{\Delta p}{q_o}\, dy$

$\dfrac{\Delta p}{q_o}$ loading coefficient (pressure on the lower surface minus pressure on the upper surface divided by free-stream dynamic pressure)

q_o free-stream dynamic pressure $\left(\tfrac{1}{2}\rho_o V_o{}^2 \right)$

q dimensionless rate of pitching $\left(\dfrac{c_o \dot{\theta}}{V_o} \right)$

s local semispan of wing

S wing area

t' time

t $a_o t'$

t_o $\dfrac{t}{c_o}$

u,v,w perturbation velocity components in the x,y,z directions, respectively

V_o free-stream velocity

x,y,z Cartesian coordinates

$x_{c.p.}$ distance of center of pressure from wing apex

α angle of attack (angle between flight path and plane of wing), radians

β $\sqrt{|1-M_o^2|}$

β_e $\dfrac{1}{m\,M_o + \sqrt{1+m^2}}$

θ wing angle of pitch, relative to initial attitude, positive when trailing edge lies below leading edge

$\dot{\theta}$ wing rate of pitch, positive when trailing edge is sinking relative to leading edge $\left(\dfrac{d\theta}{dt'}\right)$

Λ angle of sweep of leading edge, positive for sweepback

ρ_o free-stream density

τ $\dfrac{t}{s}$

τ_o chord lengths traveled $\left(\dfrac{V_o t'}{c_o} \text{ or } M_o t_o\right)$

φ perturbation velocity potential

$\Delta\varphi$ jump in potential across the $z=0$ plane $[\varphi(x,y,0^+) - \varphi(x,y,0^-)]$

Subscripts

n component taken normal to the leading edge

u positive side of the $z=0$ plane, or upper surface of a wing

THE PROBLEM AND THE NATURE

OF ITS SOLUTION

Consider a wing situated in still air and a Cartesian coordinate system with origin on the leading edge at the point of wing symmetry. At time equal to zero, the wing starts impulsively to move in a straight line with constant velocity away from the coordinate system which remains fixed relative to the still air at infinity. The load distribution on a wing undergoing such a motion is called the indicial loading. Similarly, the forces and moments which are based on this loading are given the adjective indicial. The partial differential equation that is satisfied by the velocity potential φ for such a motion can be written

$$\varphi_{tt} - \varphi_{xx} - \varphi_{yy} - \varphi_{zz} = 0 \tag{1}$$

which is the normalized form of the wave equation. In equation (1), $x, y,$ and z are distances: x measured chordwise, y spanwise, and z vertically, and t is equal to $a_0 t'$ where a_0 is the free-stream speed of sound and t' is time.

The boundary conditions to which equation (1) is subject are dependent on the wing shape and motion. Adopting the assumptions of thin-airfoil theory, which are consistent with the assumptions already used in obtaining equation (1), it can be assumed that the slope of the wing surface, in the direction of motion, at any place and time is given by the ratio of the vertical velocity component in the $z=0$ plane to the wing's forward velocity component. For a flat plate, then, the following conditions are to be satisfied:

1. The vertical velocity φ_z is a linear function of x, the coefficients of which depend upon the angle of attack and rate of pitch, over the portion of the xy plane occupied by the wing at any given time.

2. No perturbations exist at infinity.

3. There are no discontinuities in the velocity potential except over the region occupied by the wing and its vortex wake.

The problem has now been expressed as one of finding, for prescribed boundary conditions, a solution to the wave equation. It is often desirable to express the solution in terms of the loading coefficient rather than the potential function or velocity components. This coefficient can be written in its linearized form as

$$\frac{\Delta p}{q_0} = \frac{2}{V_0 M_0} \frac{\partial \Delta \varphi}{\partial t} \tag{2}$$

The solution of the problem without further restrictions has, in general, not been obtained, although it can be shown that the boundary conditions for any wing in unsteady motion can be satisfied by a suitable superposition of sources and doublets (reference 4). However, the solution for wings with all supersonic edges can be written as a double integral of sources having intensities determined by the local slope of the wing. Hence, for a flat surface at constant angle of attack and not pitching,

$$\varphi(x,y) = \frac{V_0 \alpha}{2\pi} \iint_{S_a} \frac{1}{r} \, dx_1 dy_1 \tag{3}$$

where S_a is the outline of the region of sources which can, at a given time, affect the point x,y at which the potential is being determined, r equals $\sqrt{(x-x_1)^2 + (y-y_1)^2}$, and α is the angle of attack of the wing. The area S_a has been termed the acoustic plan form and a discussion of its significance is given in reference 4.

The solution for the triangular wing with subsonic edges can be obtained in certain regions, but in others the problem reverts to the solution of a double integral equation involving time and the two surface dimensions of the wing. If the triangular wing is slender, an approximate method for finding the pressure over the entire wing can be used. This method is to neglect the streamwise velocity gradients in comparison with the gradients in the plane normal to the free stream and also in comparison with the term φ_{tt}. There results for the partial differential equation governing the flow field (equation (1)) the wave equation of one lower dimension, namely,

$$\varphi_{tt} - \varphi_{yy} - \varphi_{zz} = 0 \tag{4}$$

As will be developed later, the boundary conditions become the same as for a rectangular flat plate of very low aspect ratio inclined at angle of attack to a free stream with a Mach number equal to $\sqrt{2}$. This analogy with the steady-state lifting-surface problem is useful since solutions to the latter problem have been obtained.

The indicial lift and pitching-moment coefficients will be determined for wings with two different vertical velocity distributions. The first is the case in which the boundary condition is

$$w_u = \varphi_z \big|_{z=0} = -V_0 \alpha$$

where α is the angle of attack, and w_u is constant over the plan form. This case is referred to as that of the sinking wing. The other boundary-value problem considered is the one corresponding to a flat wing pitching at a constant rate about its leading edge or apex. The boundary conditions have the form

$$w_u = \varphi_z\big|_{z=0} = -\dot{\theta}\,(x + M_0 t)$$

where θ is the constant rate of pitch and $(x + M_0 t)$ is the distance aft the leading edge or apex of the wing. The pitching velocity $\dot{\theta}$ is considered positive when the trailing edge of the wing sinks relative to the axis of rotation.

The difference between α and θ is illustrated in the sketch, where for clearness the motion is shown to be oscillatory rather than indicial. The angle of attack α is the angle between the flat wing surface and the line tangent to the flight path of the leading edge or apex of the wing. The angle θ is the angle between the flat wing surface and the horizontal (see part (a) of the sketch). Part (b) of the sketch shows a wing undergoing a sinusoidal angle-of-attack variation with a zero angle of pitch throughout the motion. Part (c.) shows a wing undergoing a sinusoidal angle-of-pitch variation taken about the leading edge, with the angle of attack remaining zero.

Direction of wing motion

Flight path of leading edge

Wing

(a)

$\theta = \dot{\theta} = 0$
$a = \sin \omega t'$

(b)

$\theta = \sin \omega t'$
$a = 0$

(c)

Although the lift and pitching-moment coefficients are given only for the two types of motion separately, it is possible, according to the linear theory, to combine them to simulate an arbitrary indicial maneuver consisting of both sinking and pitching motions. For such a case, the boundary condition becomes

$$w_u = -V_0 \alpha - \dot{\theta}\,(x + M_0 t)$$
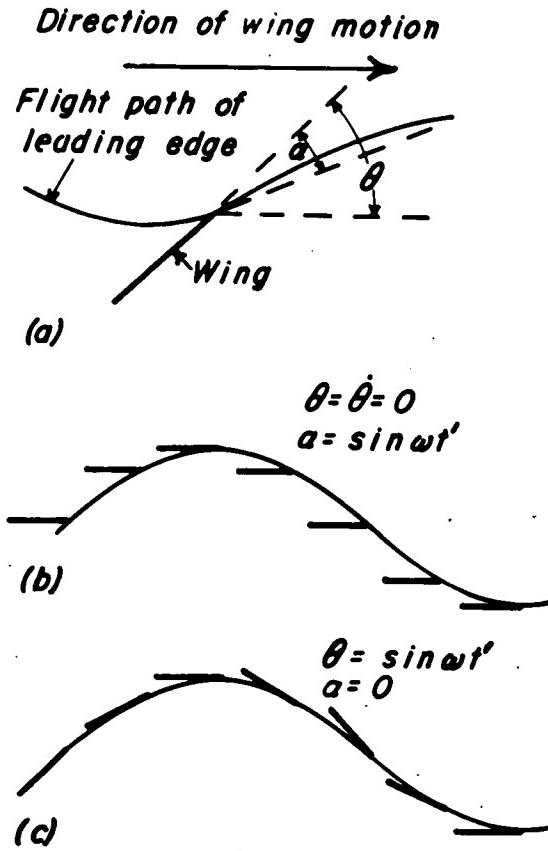
If, furthermore, the desired maneuver is not indicial, the lift and pitching-moment coefficients may be determined by use of Duhamel's integral:

$$C_L = \frac{d}{dt'} \int_0^{t'} [C_{L_\alpha}(t'-\tau') \, \alpha(\tau') + C_{L_q}'(t'-\tau')q(\tau')] \, d\tau'$$

$$C_m = \frac{d}{dt'} \int_0^{t'} [C_{m_\alpha}'(t'-\tau')\alpha(\tau') + C_{m_q}'(t'-\tau') \, q(\tau')] \, d\tau'$$

where $\alpha(t')$ and $q(t')$ are the arbitrary motions $\left(q = \frac{c_0 \dot{\theta}}{V_0}\right)$, C_{L_α}, C_{m_α}', C_{L_q}', and C_{m_q}' are the indicial aerodynamic coefficients, and the primes on the coefficients indicate that the pitching motion is about, and the pitching moments are referred to, the leading edge or apex.

The position of the axis of pitching motion, and of the axis to which pitching-moment coefficient is referred, is of importance. In this report, these axes coincide in an axis normal to the root chord of the wing and passing through the wing leading edge or apex. However, it is often desired to transfer the pitching motion and moment calculation to other axes, and the formulas for such a transformation will be given here. Let the pitching motion refer to an axis lying a distance ac_0 back of the leading edge or apex, and let the pitching-moment coefficients refer to an axis bc_0 aft the leading edge or apex. The necessary transformation formulas are

$$C_{m_\alpha}\big|_b = C_{m_\alpha}' + b \, C_{L_\alpha}$$

$$C_{L_q}\big|_a = C_{L_q}' - a \, C_{L_\alpha}$$

$$C_{m_q}\big|_{a,b} = C_{m_q}' + b \, C_{L_q}' - a \, C_{m_\alpha}' - ab \, C_{L_\alpha}$$

where a prime on a quantity indicates that the pitching motion is about, and the pitching moments are measured about, an axis through the leading edge or apex of the wing. The quantity q is the dimensionless rate of pitching, equal to $c_0 \dot{\theta}/V_0$. The subscripts a and b mean, respectively, that the quantity in question refers to a pitching motion about an axis at a distance ac_0 aft the leading edge or apex, or that the pitching moments are measured about an axis bc_0 aft the leading edge or apex.

WING   WITH   SUPERSONIC   EDGES

INDICIAL LOADING FOR SINKING WING

Analysis

The seven regions.— The analytic expression for the indicial load-
ing over the triangular wing has a different form in each of seven
regions. These regions are determined by the positions of the various
wave fronts relative to the wing plan form (fig. 1). For $t < 0$ the
wing is motionless, its leading edge lying along lines represented by
the dashed lines in figure 1. At $t=0$ the wing starts suddenly to
move, and for $t > 0$, travels forward at a constant speed V_0. After a
certain time t has elapsed, the wing has traveled to a new position,
also shown in the figure. In this same interval of time, pressure
impulses have traveled out in spherical waves from every point of the
region which the wing has occupied. The trace on the wing of the
sphere starting from the wing apex at $t=0$ forms the external boundary
of region 7. The area outside this circle and within the traces of the
cylindrical waves (the envelopes of the spherical waves) generated by
the leading edges at $t=0$ forms region 4. Region 5 is formed by the
overlapping of these cylindrical waves, and the solution for loading
within it can be found by a suitable superposition of the solutions for
regions 3 and 4. Region 1 lies between the cylinder trace on the wing
and the leading—edge position at time t; the loading in this region
cannot be affected by the manner in which the wing started its motion
since it lies outside the starting cylindrical waves. Hence, the
loading in region 1 is the same as that on a swept wing flying at a
steady supersonic speed. The solution in region 2 can also be obtained
from steady—state lifting—surface theory, but, whereas in region 1 the
field is two—dimensional (i.e., invariant with distance measured parallel
to the leading edge), in region 2 the field is conical. Region 6 is
formed by the overlapping of regions 2 and 4. Finally, region 3 is that
area completely unaffected by waves from the wing edges. In the follow-
ing subdivisions the analysis of each of the separate regions will be
discussed.

Region 1: The loading in region 1 of figure 1 is equal to the
loading on a two—dimensional flat plate moving at a constant velocity
given by the component of stream velocity normal to the leading edge
of the triangular wing. Since this component is supersonic, the
loading is of the Ackeret type and is given by

$$\left(\frac{\Delta p}{q_n}\right)_1 = \frac{4\alpha_n}{\beta n}$$

But since $V_n = V_0 \cos \Lambda$ where Λ is the angle of sweep (see fig. 2),

$$q_n = q_0 \cos^2 \Lambda$$

$$c_n = \alpha \ \sec \ \Lambda$$

$$M_n = M_0 \cos \Lambda$$

$$\beta_n = \sqrt{M_0^2 \cos^2 \Lambda - 1}$$

and

$$\left(\frac{\Delta p}{q_0}\right)_1 = \frac{4\alpha}{\sqrt{M_0^2 - \sec^2 \Lambda}}$$

Finally, if $\ ctn \ \Lambda = m$

$$\left(\frac{\Delta p}{q_0}\right)_1 = \frac{4\alpha m}{\sqrt{\beta^2 m^2 - 1}} \tag{5}$$

where $\ \beta = \sqrt{M_0^2 - 1}.$

Region 2: The steady—state loading on a triangular wing with supersonic edges has been given by several authors (see, for conven—. ience, reference 5) so the expression for the loading in region 2 can be written immediately for the coordinate system shown in figure 2 as

$$\left(\frac{\Delta p}{q_0}\right)_2 = \frac{4\alpha m}{\pi \sqrt{\beta^2 m^2 - 1}} \left\{ \pi + \arcsin \frac{\beta^2 my - (x + M_0 t)}{\beta[m(x + M_0 t) - y]} - \right.$$

$$\left. \arcsin \ \frac{\beta^2 my + (x + M_0 t)}{\beta[M(x + M_0 t) + y]} \right\} \tag{6}$$

Region 3: Since region 3 is unaffected by the edges of the wing the solution for the loading therein can be written as in reference 6

$$\left(\frac{\Delta p}{q_0}\right)_3 = \frac{4\alpha}{M_0} \tag{7}$$

Region 4: The solution for loading in region 4 can be obtained from consideration of a two—dimensional wing starting from rest and moving with velocity V_n normal to its leading edge. This problem

has been treated in reference 6 and the solution written there can be written for the right-hand side of figure 1 as

$$\left(\frac{\Delta p}{q_n}\right)_4 = \frac{4a_n}{\pi \beta_n}\left[\text{ arc cos }\frac{M_n x_n + t}{x_n + M_n t} + \frac{\sqrt{M_n^2 - 1}}{M_n}\left(\frac{\pi}{2} + \text{arc sin }\frac{x_n}{t}\right)\right]$$

where the notation, as defined by the sketch, is

$$x_n = x \cos \Lambda - y \sin \Lambda$$

$$y_n = x \sin \Lambda + y \cos \Lambda$$

and since

$$\text{ctn }\Lambda = m, \quad \sin \Lambda = \frac{1}{\sqrt{1+m^2}},$$

$$\cos \Lambda = \frac{m}{\sqrt{1+m^2}}$$

Then

$$x_n = \frac{mx - y}{\sqrt{1+m^2}}$$

$$y_n = \frac{x + my}{\sqrt{1+m^2}}$$
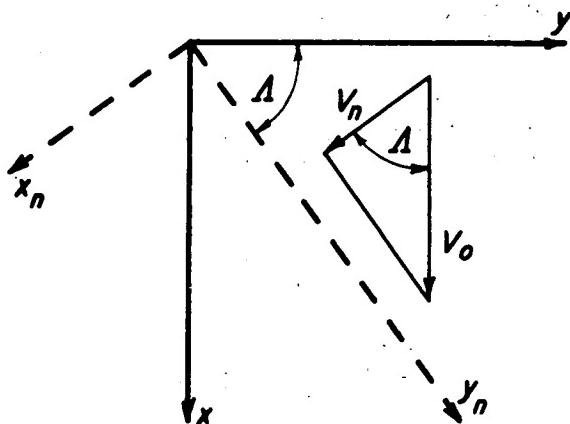
The equation for loading now becomes, in the coordinate system of figure 2,

$$\left(\frac{\Delta p}{q_o}\right)_4 = \frac{4am}{\pi\sqrt{\beta^2 m^2 - 1}}\left[\text{arc cos }\frac{mM_o(mx - |y|) + t(1+m^2)}{\sqrt{1+m^2}\,(mx - |y| + mM_o t)} + \right.$$

$$\left.\frac{\sqrt{\beta^2 m^2 - 1}}{mM_o}\left(\frac{\pi}{2} + \text{arc sin }\frac{mx - |y|}{t\sqrt{1+m^2}}\right)\right] \tag{8}$$

Region 5: The solution for loading in region 5 can be obtained by superposition of the solutions for regions 3 and 4. If the solutions for the two sides of region 4 (obtained from equation 8) are added, the result gives a value of w_u of twice the required amount in region 5, as well as undesirable pressures off the wing. However, subtraction from this sum of the solution for region 3 (equation 7) reduces the downwash w_u to the proper value, and also cancels the excess pressures. The resulting expression can be written

$$\left(\frac{\Delta p}{q_0}\right)_5 = \frac{4\alpha m}{\pi\sqrt{\beta^2 m^2-1}}\left[\text{arc cos }\frac{mM_0(mx-y)+(1+m^2)t}{\sqrt{1+m^2}\,(mx-y+mM_0 t)}\right.+$$

$$\text{arc cos }\frac{mM_0(mx+y)+(1+m^2)t}{\sqrt{1+m^2}\,(mx+y+mM_0 t)}+$$

$$\left.\frac{\sqrt{\beta^2 m^2-1}}{mM_0}\left(\text{arc sin }\frac{mx+y}{\sqrt{1+m^2}\,t}+\text{arc sin }\frac{mx-y}{\sqrt{1+m^2}\,t}\right)\right]\quad(9)$$

Region 6: The loading in region 6 can also be calculated by superposition. To find the loading in this case, add the solutions for regions 2 and 4 (equations (6) and (8)) and subtract the solution for region 1 (equation (5)). There results

$$\left(\frac{\Delta p}{q_0}\right)_6 = \frac{4\alpha m}{\pi\sqrt{\beta^2 m^2-1}}\left\{\text{arc sin }\frac{\beta^2 my-(x+M_0 t)}{\beta[m(x+M_0 t)-y]}-\text{arc sin }\frac{\beta^2 my+(x+M_0 t)}{\beta[m(x+M_0 t)+y]}\right.+$$

$$\text{arc cos }\frac{mM_0(mx-|y|)+t(1+m^2)}{(mx-|y|+mM_0 t)\sqrt{1+m^2}}+$$

$$\left.\frac{\sqrt{\beta^2 m^2-1}}{mM_0}\left(\frac{\pi}{2}+\text{arc sin }\frac{mx-|y|}{t\sqrt{1+m^2}}\right)\right\}\quad(10)$$

Region 7: The solution for the loading in region 7 can be obtained by means of equation (3). The analysis used in finding the solution in this region is not difficult but the algebra is rather involved. It is useful at this point to introduce polar coordinates (see sketch) such that
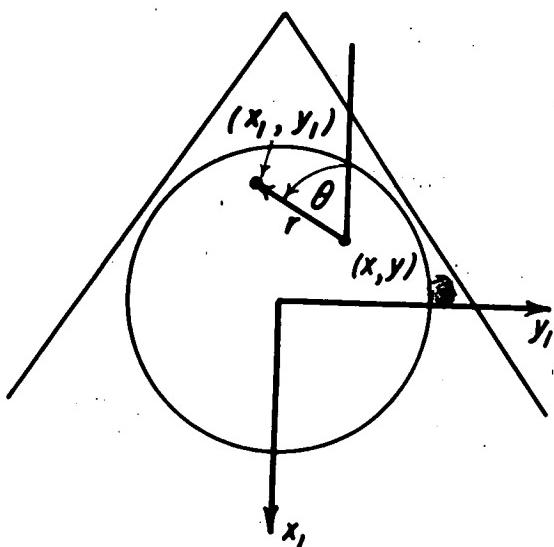

$$x-x_1 = r\cos\theta$$

$$y-y_1 = r\sin\theta$$

$$dx_1 dy_1 = r\,dr\,d\theta\quad(11)$$

From equation (11), equation (3) can be written in the form

$$\varphi = \frac{V_0\alpha}{2\pi}\int_{S_a}\int dr\,d\theta\quad(12)$$
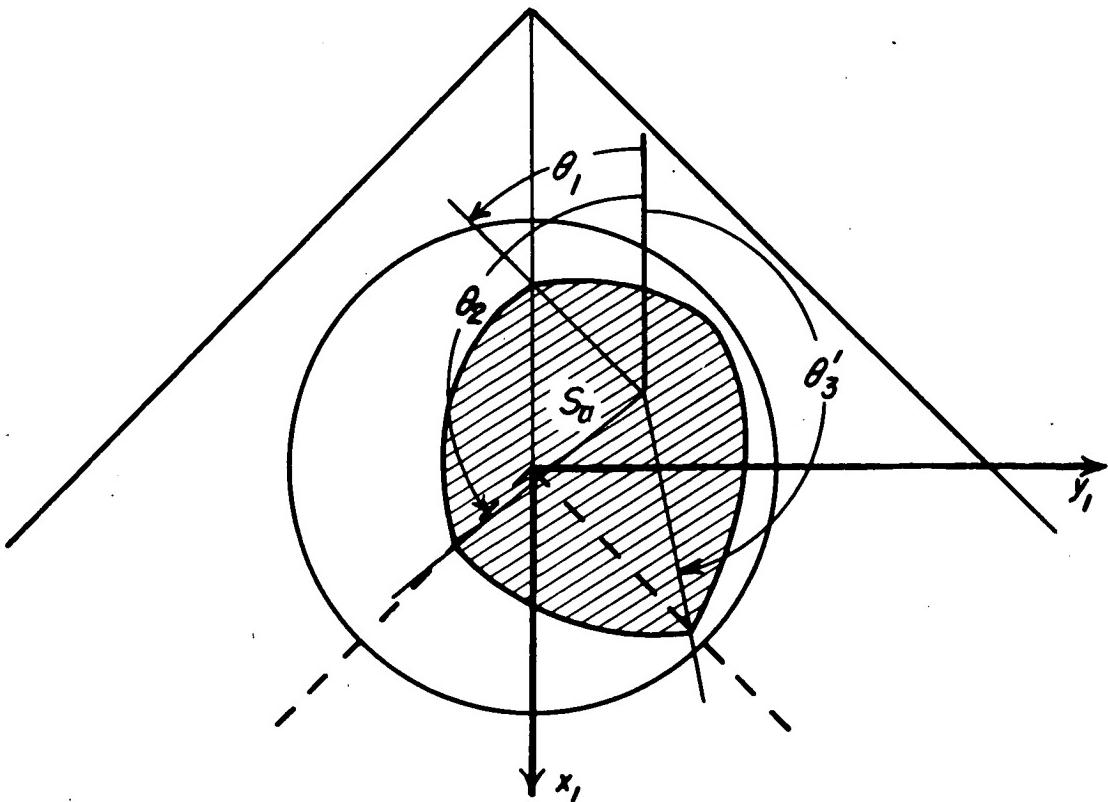
The acoustic plan form for points in region 7 is the region
bounded by three curves as indicated in the sketch. The arc between
θ_1 and θ_2 is determined by eliminating T between the equations

$$r^2 = (t - T)^2$$

(the equation for the inverse sound waves) and the equation for the
left leading edge

$$y_1 = -m(x_1 + M_0 T)$$

The arc between θ_3 and θ_1 is found by determining the acoustic
intersection (eliminating T) of the right leading edge with the
inverse sound wave; and, finally, the arc between θ_2 and θ_3 is
given by the equation r=t. The equations of these arcs can be
written in polar coordinates as

$$r = \frac{m(x+M_O t)+y}{m \cos \theta + mM_O + \sin \theta} \quad ; \quad \theta_1 \le \theta \le \theta_2$$

$$r = t; \quad \theta_2 \le \theta \le \theta_3$$

$$r = \frac{m(x+M_O t)-y}{m \cos \theta + mM_O - \sin \theta} \quad ; \quad \begin{cases} 0 \le \theta \le \theta_1 \\ \theta_3 \le \theta \le 2\pi \end{cases}$$

Using these expressions, equation (12) reduces to

$$\varphi = \frac{V_O \alpha}{2\pi} \int_{\theta_1}^{\theta_2} \frac{m(x+M_O t)+y}{m \cos \theta + mM_O + \sin \theta} \, d\theta +$$

$$\frac{V_O \alpha}{2\pi} \int_{\theta_2}^{\theta_3} t \, d\theta +$$

$$\frac{V_O \alpha}{2\pi} \int_{\theta_3}^{\theta_1} \frac{m(x+M_O t)-y}{m \cos \theta + mM_O - \sin \theta} \, d\theta$$

and taking the partial derivative with respect to t (to determine the loading according to equation (2)) one finds[1]

$$\left(\frac{\Delta p}{q_O}\right)_7 = \frac{2\alpha \, m}{\pi} \int_{\theta_1}^{\theta_2} \frac{d\theta}{mM_O + m \cos \theta + \sin \theta} + \frac{2\alpha}{\pi M_O} \int_{\theta_2}^{\theta_3} d\theta +$$

$$\frac{2\alpha \, m}{\pi} \int_{\theta_3}^{\theta_1} \frac{d\theta}{mM_O + m \cos \theta - \sin \theta} \qquad (13)$$

In evaluating this equation, the following integral is used:

for $-\pi \le \theta \le \pi$

$$\int \frac{d\theta}{mM_O + m \cos \theta \pm \sin \theta} = \frac{2}{\sqrt{\beta^2 m^2 - 1}} \arctan \frac{m(M_O - 1)\tan(\theta/2) \pm 1}{\sqrt{\beta^2 m^2 - 1}} \qquad (14)$$

---

[1]The limits θ_1, θ_2, and θ_3 are all functions of t but in moving the partial derivative through the integral sign the terms involving $\partial\theta_1/\partial t$, $\partial\theta_2/\partial t$, and $\partial\theta_3/\partial t$ all cancel one another.

Since equation (14) is valid only in the interval $-\pi \leq \theta \leq \pi$, care must be exercised in applying it because the angle θ_3 may be greater than π (as in the preceding sketch). In case $\pi \leq \theta_3$, it is convenient to introduce the angle $\theta_3' = \theta_3 - 2\pi$. The expression for $\Delta p / q_0$ can then be written in two forms, according as θ_3 is less than or greater than π:

for $y \geq 0$, $\theta_3 \leq \pi$

$$\left(\frac{\Delta p}{q_0}\right)_7 = \frac{4\alpha m}{\pi \sqrt{\beta^2 m^2 - 1}} \left[\pi + \arctan \frac{m(M_0-1)\tan(\theta_1/2)-1}{\sqrt{\beta^2 m^2 - 1}} - \right.$$

$$\arctan \frac{m(M_0-1)\tan(\theta_1/2)+1}{\sqrt{\beta^2 m^2 - 1}} + \arctan \frac{m(M_0-1)\tan(\theta_2/2)+1}{\sqrt{\beta^2 m^2 - 1}} -$$

$$\left. \arctan \frac{m(M_0-1)\tan(\theta_3/2)-1}{\sqrt{\beta^2 m^2 - 1}} \right] + \frac{2\alpha}{\pi M_0}(\theta_3 - \theta_2) \qquad (15a)$$

for $y \geq 0$, $\pi \leq \theta_3$

$$\left(\frac{\Delta p}{q_0}\right)_7 = \frac{4\alpha m}{\pi \sqrt{\beta^2 m^2 - 1}} \left[\arctan \frac{m(M_0-1)\tan(\theta_1/2)-1}{\sqrt{\beta^2 m^2 - 1}} - \right.$$

$$\arctan \frac{m(M_0-1)\tan(\theta_1/2)+1}{\sqrt{\beta^2 m^2 - 1}} + \arctan \frac{m(M_0-1)\tan(\theta_2/2)+1}{\sqrt{\beta^2 m^2 - 1}} -$$

$$\left. \arctan \frac{m(M_0-1)\tan(\theta_3'/2)-1}{\sqrt{\beta^2 m^2 - 1}} \right] + \frac{2\alpha}{\pi M_0}(\theta_3' - \theta_2 + 2\pi) \qquad (15b)$$

where

$$\theta_1 = \arccos \frac{-M_0 y^2 + (x+M_0 t)\sqrt{(x+M_0 t)^2 - \beta^2 y^2}}{y^2 + (x+M_0 t)^2}$$

$$(0 < \theta_1 < \pi)$$

$$\theta_2 = \arccos \frac{m(y+mx) - \sqrt{(1+m^2)t^2 - (y+mx)^2}}{(1+m^2)t}$$

$$(0 < \theta_2 < \pi)$$

$$\theta_3 = \text{arc cos } \frac{-m(y-mx) - \sqrt{(1+m^2)t^2 - (y-mx)^2}}{(1+m^2)\ t}$$

$$\theta_3' = \theta_3 - 2\pi \quad (\text{if } \pi \leq \theta_3)$$

The limitation on θ_3 can be given both an analytic and geometric interpretation. Thus, equation (15(a)) applies for $0 \leq m(x+t) \leq y$ and equation (15(b)) applies for $0 \leq y \leq m(x+t)$. These regions are shown in the accompanying sketch. Because of the geometrical symmetry about the x axis, equations (15) suffice for the determination of loading throughout region 7.
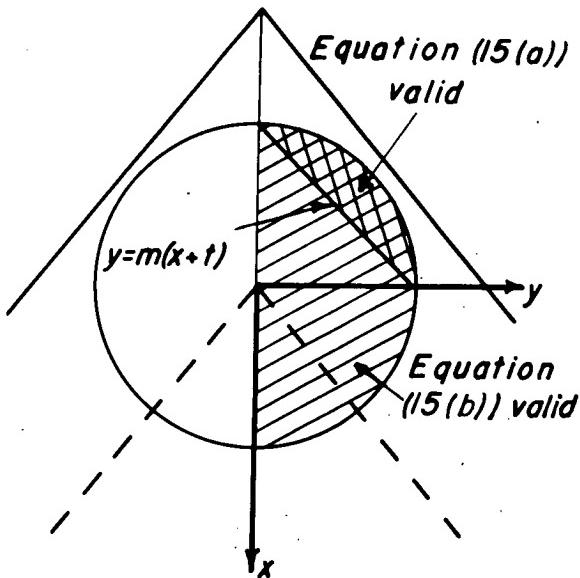
Discussion of Results

Plots of the load distribution on the sinking triangular wing with supersonic edges are shown in figure 3, and an isometric drawing of the

loading on the right panel appears
in the sketch. The positions of
the spanwise sections were chosen
so that each of the regions 1
through 7 is represented. It is
to be noted that the results for
region 7 show no unusual charac-
teristics, but fit in well with
those for the adjoining regions.
In general, the distribution is
similar to the steady-state load-
ing on a triangular wing.

INDICIAL LIFT AND

PITCHING MOMENT

Analysis
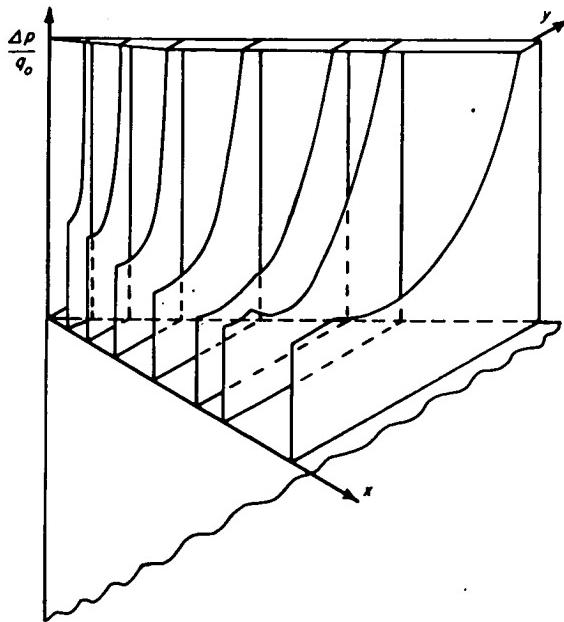
Methods of solution.— If a
detailed knowledge of the load
distribution is not required, but only the total values of lift and
moment need be known, analyses much simpler than the one presented in
the previous section can be employed. These methods, however, not only
require the edges of the wing to be supersonic, but also require the
trailing edge to be straight and normal to the free-stream direction.
One such simple method has been presented in reference 4. It involves
the integration over the three-dimensional plan form of longitudinal
strips, or elements, which carry the two-dimensional values of loading
as a function of time. The results presented in the present section
can be derived by this method as well as by the method to be developed
next.

Consider again equation (1) and integrate each term with respect
to y between the limits minus and plus infinity.[2] There results the
equation

$$\int_{-\infty}^{\infty} \frac{\partial^2 \varphi}{\partial x^2} \, dy + \int_{-\infty}^{\infty} \frac{\partial^2 \varphi}{\partial y^2} \, dy + \int_{-\infty}^{\infty} \frac{\partial^2 \varphi}{\partial z^2} \, dy - \int_{-\infty}^{\infty} \frac{\partial^2 \varphi}{\partial t^2} \, dy = 0$$

If $y = y_l(x,z,t)$ and $y = y_r(x,z,t)$ are the equations of the Mach
waves streaming back from the leading edges on the left and right sides
of the wing, respectively, then, since φ is continuous across these

[2]The basic idea for this solution was given by Prof. P. A. Lagerstrom
in his lectures at the California Institute of Technology.

waves but φ_x, φ_y, φ_z, and φ_t are not,

$$\frac{\partial^2}{\partial x^2} \int_{y_l}^{y_r} \varphi \, dy = \frac{\partial y_r}{\partial x} u_r - \frac{\partial y_l}{\partial x} u_l + \int_{y_l}^{y_r} \frac{\partial^2 \varphi}{\partial x^2} \, dy$$

where u_r and u_l are the values of u on the interior faces of the right and left Mach waves, respectively, and

$$\int_{y_l}^{y_r} \frac{\partial^2 \varphi}{\partial y^2} \, dy = v_r - v_l$$

Values of the terms involving w and φ_t are similar to those involving u so that finally, if

$$\Phi = \int_{y_l}^{y_r} \varphi \, dy \tag{16}$$

then

$$\frac{\partial^2 \Phi}{\partial x^2} + \frac{\partial^2 \Phi}{\partial z^2} - \frac{\partial^2 \Phi}{\partial t^2} = \left(\frac{\partial y_r}{\partial x} u_r + \frac{\partial y_r}{\partial z} w_r - \frac{\partial y_r}{\partial t} \varphi_t - v_r \right) -$$

$$\left(\frac{\partial y_l}{\partial x} u_l + \frac{\partial y_l}{\partial z} w_l - \frac{\partial y_l}{\partial t} \varphi_t - v_l \right)$$

The terms enclosed within the brackets in the last equation combine so that each bracketed quantity is zero. For the case of interest here, this is not difficult to show. Consider, for example, the right wedge. Then, since the equation of the wedge is

$$y_r = -z \sqrt{\beta^2 m^2 - 1} + mx + mM_0 t$$

and the value of the potential is the steady-state two-dimensional value given by the expression

$$\varphi_r = -w_u \frac{m(x + M_0 t) - y - z \sqrt{\beta^2 m^2 - 1}}{\sqrt{\beta^2 m^2 - 1}}$$

the term

$$\left(\frac{\partial y_r}{\partial x} u_r + \frac{\partial y_r}{\partial z} w_r - \frac{\partial y_r}{\partial t} \varphi_t - v_r \right)$$

becomes

$$-w_u \left(m \frac{m}{\sqrt{\beta^2 m^2 - 1}} + \sqrt{\beta^2 m^2 - 1} - \frac{m^2 M_o^2}{\sqrt{\beta^2 m^2 - 1}} + \frac{1}{\sqrt{\beta^2 m^2 - 1}} \right)$$

and this is identically zero.[3]

Finally, therefore, equation (1) has been reduced in terms of equation (16) to

$$\Phi_{tt} - \Phi_{xx} - \Phi_{zz} = 0 \tag{17}$$

Consider next the boundary conditions for a triangular wing with supersonic edges. In the plane $z=0$, $\partial \Phi / \partial z$ becomes $\displaystyle\int_{-\infty}^{\infty} w_u dy$ where w_u is the vertical induced velocity in the plane of the wing. Since the edges are supersonic, however, w_u must be zero off the plan form of the wing and the integration need extend only over the plan form itself. Hence

$$\left(\frac{\partial \Phi}{\partial z} \right)_{z=0} = -2V_o \alpha m \ (x + M_o t) \tag{18}$$

for the flat triangular wing at constant angle of attack and

$$\left(\frac{\partial \Phi}{\partial z} \right)_{z=0} = -2\dot{\theta} m \ (x + M_o t)^2 \tag{19}$$

---

[3]It is not necessary to perform a direct calculation in order to prove the above result for arbitrary plan forms. The bracketed terms represent the directional derivative of the velocity potential taken along the so-called "conormal" of the foremost disturbance surface. Since φ is constant on the surface, and since the conormal lies along the surface, the bracketed terms are zero.

for a flat triangular wing with a constant rate of pitch θ about its apex (positive $\dot\theta$ produces a downward motion of the trailing edge relative to the leading edge).
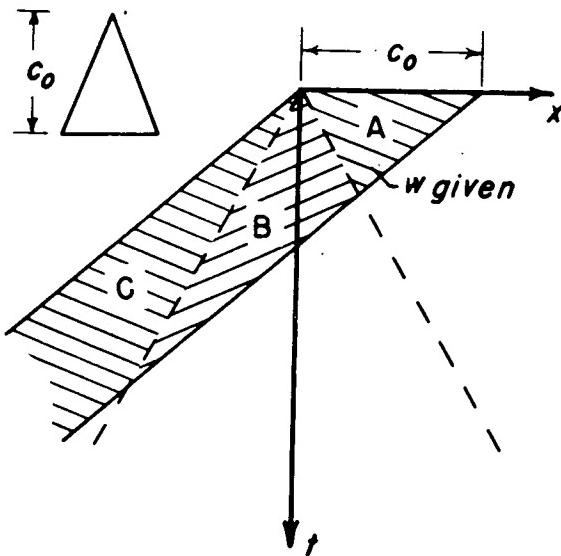
These boundary conditions are exactly like those studied in steady-state supersonic wing theory. In fact, the lifting-surface analog (shown on the sketch) is a wing tip of specified camber in a supersonic free stream having a Mach number equal to $\sqrt{2}$. The solution for the potential in the plane of the wing for this problem can therefore be written immediately as

$$(\Phi)_{z=0} = -\frac{1}{\pi} \int_\sigma \int \frac{\left(\dfrac{\partial \Phi}{\partial z}\right)_{z=0}}{\sqrt{(t-t_1)^2 - (x-x_1)^2}} \, dt_1 \, dx_1$$

where σ is the portion of the area on the shaded surface in the sketch lying ahead of the forecone traces given by the equation $(t-t_1)^2 = (x-x_1)^2$. Using equation (2) for the loading coefficient, and introducing the following notation for the average spanwise loading

$$P_0 = \frac{M_0}{2s\alpha} \int_{-s}^{s} \frac{\Delta p}{q_0} dy \quad \text{(sinking wing)} \qquad (20a)$$

$$P_1 = \frac{m M_0 V_0}{2s^2 \dot\theta} \int_{-s}^{s} \frac{\Delta p}{q_0} dy \quad \text{(pitching wing)} \qquad (20b)$$

where

$$s = m(x+M_0 t) \qquad (21)$$

it is found that

$$P_0 = \frac{4m}{\pi s} \frac{\partial}{\partial t} \int_\sigma \int \frac{(x_1+M_0 t_1)\, dx_1 dt_1}{\sqrt{(t-t_1)^2 - (x-x_1)^2}} \qquad (22)$$

$$P_1 = \frac{4m^2}{\pi s^2} \frac{\partial}{\partial t} \int_\sigma \int \frac{(x_1+M_0 t_1)^2\, dx_1\, dt_1}{\sqrt{(t-t_1)^2 - (x-x_1)^2}} \qquad (23)$$

Wing with constant angle of attack (sinking wing).— The solution for the average load on a flat, supersonic–edged, triangular wing starting from rest at $t=0$ and flying at a constant speed and angle of attack is given by equation (22). With the transformations

$$x-x_1 = x_2$$

$$t-t_1 = t_2$$

this becomes

$$P_0 = \frac{4m}{\pi s} \frac{\partial}{\partial t} \int_\sigma \int dt_2 dx_2 \frac{\frac{s}{m} - x_2 - M_0 t_2}{\sqrt{t_2^2 - x_2^2}}$$

This integral can be evaluated and gives for $x < t$ (region A)

$$P_0 = 4 \qquad (24a)$$

for $-t \leq x \leq t$ (region B)

$$P_0 = \frac{4}{\pi} \left[\frac{\sqrt{t^2-x^2}}{x+M_0 t} + \text{arc } \cos\left(-\frac{x}{t}\right) + \frac{M_0}{\beta} \text{arc } \cos \frac{t+M_0 x}{x+M_0 t} \right] \qquad (24b)$$

and for $x < -t$ (region C)

$$P_0 = \frac{4M_0}{\beta} \qquad (24c)$$

where the regions are shown in the preceding sketch. Equations (24) can also be obtained by integrating the equations for the loading given in

the preceding section. These integrations were carried out (in some regions numerically) and the results were found to agree with those of the present analysis.

It is now possible to write the equation for the indicial lift and pitching moment for a sinking wing:

$$C_{L_\alpha} = \frac{2}{S\,M_0} \int_{-M_0 t}^{c_0-M_0 t} m(x+M_0 t)\,P_0\,dx \qquad (25)$$

$$C_{m_\alpha}' = -\frac{2}{S\,c_0\,M_0} \int_{-M_0 t}^{c_0-M_0 t} m(x+M_0 t)^2\,P_0\,dx \qquad (26)$$

where S is the wing area (equal to mc_0^2) and the prime indicates that the pitching moment is measured about the apex, the positive moment being one which causes the trailing edge to sink relative to the apex.

Combining equations (24) and (25) one finds for the first interval shown in the sketch
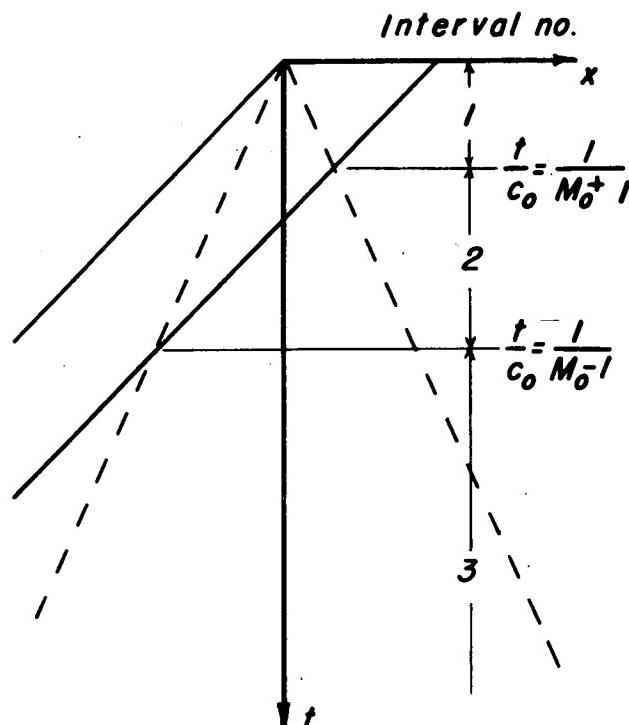
$$C_{L_\alpha} = \frac{2}{M_o c_o^2} \left\{ \int_{-Mt}^{-t} \frac{4M_o}{\beta} (x + M_o t) \, dx + \right.$$

$$\frac{4}{\pi} \int_{-t}^{t} (x + M_o t) \left[\frac{\sqrt{t^2 - x^2}}{x + M_o t} + \text{arc cos} \left(-\frac{x}{t} \right) + \right.$$

$$\left. \frac{M_o}{\beta} \text{ arc cos } \frac{t + M_o x}{x + M_o t} \right] \, dx +$$

$$\left. \int_{t}^{c_o - M_o t} 4(x + M_o t) \, dx \right\}$$

This equation integrates to give, if $t_o = t/c_o$,

for $0 \le t_o \le \frac{1}{M_o + 1}$ (first interval)

$$C_{L_\alpha} = \frac{4}{M_o} \left(1 + \frac{1}{2} t_o^2 \right) \tag{27a}$$

Similarly for $\frac{1}{M_o + 1} \le t_o \le \frac{1}{M_o - 1}$ (second interval)

$$C_{L_\alpha} = \frac{4}{\pi M_o} \left(1 + \frac{1}{2} t_o^2 \right) \text{arc cos } \frac{M_o t_o - 1}{t_o} +$$

$$\frac{4}{\pi \beta} \text{arc cos } (M_o - t_o \beta^2) +$$

$$2 \frac{3 - M_o t_o}{\pi M_o} \sqrt{t_o^2 - (1 - M_o t_o)^2} \tag{27b}$$

and for $\frac{1}{M_o - 1} \le t_o$ (third interval)

$$C_{L_\alpha} = \frac{4}{\beta} \tag{27c}$$

In the same manner the values for $C_{m_\alpha}{}'$ in the various intervals can be determined by combining equations (24) and (26). There results

for $0 \leq t_0 \leq \dfrac{1}{M_0+1}$ (first interval)

$$C_{m_\alpha}{}' = -\frac{8}{3M_0}\left(1 + \frac{1}{2}M_0 t_0{}^3\right) \tag{28a}$$

for $\dfrac{1}{M_0+1} \leq t_0 \leq \dfrac{1}{M_0-1}$ (second interval)

$$C_{m_\alpha}{}' = -\frac{8}{\pi M_0}\left[\frac{1}{18}\,(8-M_0 t_0-M_0{}^2 t_0{}^2-2t_0{}^2)\,\sqrt{t_0{}^2-(1-M_0 t_0)^2}\;+\right.$$

$$\left.\frac{1}{6}\,(2+M_0 t_0{}^3)\;\text{arc cos}\;\frac{M_0 t_0-1}{t_0} + \frac{M_0}{3\beta}\;\text{arc cos}\;(M_0-\beta^2 t_0)\right] \tag{28b}$$

and for $\dfrac{1}{M_0-1} \leq t_0$ (third interval)

$$C_{m_\alpha}{}' = -\frac{8}{3\beta} \tag{28c}$$

Numerical results for a Mach number of 2 will be presented in the discussion section.

<u>Wing with linear angle-of-attack variation (pitching wing)</u>.— The solution for the average load on a flat, supersonic-edged, triangular wing flying at a constant speed and pitching at a uniform rate $\dot{\theta}$ about its apex is given by equation (23). With the transformation

$$x-x_1 = x_2$$

$$t-t_1 = t_2$$

this equation becomes

$$P_1 = \frac{4m^2}{\pi s^2}\frac{\partial}{\partial t}\int_\sigma \int \frac{\left(\frac{s}{m} - x_2 - M_0 t_2\right)^2}{\sqrt{t_2{}^2 - x_2{}^2}}\;dt_2\;dx_2$$

and the evaluation of this gives (for the regions defined for the sinking wing)

for $x \leq t$ (region A)

$$P_1 = 4 \left[1 + \frac{1}{2} \left(\frac{t}{x+M_0 t} \right)^2 \right] \qquad (29a)$$

for $-t \leq x \leq t$ (region B)

$$P_1 = \frac{4}{\pi} \left[\frac{1}{2} \frac{t^2 + (x+M_0 t)^2}{(x+M_0 t)^2} \text{ arc cos } \left(-\frac{x}{t} \right) + \right.$$

$$\left. \frac{M_0}{\beta} \text{ arc cos } \frac{t+M_0 x}{x+M_0 t} + \frac{1}{2} \frac{3x+2M_0 t}{(x+M_0 t)^2} \sqrt{t^2-x^2} \right] \qquad (29b)$$

and for $x \leq -t$ (region C)

$$P_1 = \frac{4M_0}{\beta} \qquad (29c)$$

The equations for lift and pitching moment on a pitching wing can be obtained from the equations

$$\frac{C_L'}{\left(\frac{c_0 \dot{\theta}}{V_0} \right)} = C_{L_q}' = \frac{2}{S c_0 M_0} \int_{-M_0 t}^{c_0 - M_0 t} m(x+M_0 t)^2 P_1 \, dx \qquad (30)$$

$$\frac{C_m'}{\left(\frac{c_0 \dot{\theta}}{V_0} \right)} = C_{m_q}' = -\frac{2}{S c_0^2 M_0} \int_{-M_0 t}^{c_0 - M_0 t} m(x+M_0 t)^3 P_1 \, dx \qquad (31)$$

where the primes indicate the wing is pitching about and the moments are measured about the leading edge.

A combination of equations (29) and (30) gives for the lift coefficient

for $0 \leq t_0 \leq \frac{1}{M_0 + 1}$ (first interval)

$$C_{T_{-}}' = \frac{8}{3M_0} \left(1 + \frac{3}{2} t_0^2 - M_0 t_0^3 \right) \tag{32a}$$

for $\frac{1}{M_0+1} \leq t \leq \frac{1}{M_0-1}$ (second interval)

$$C_{L_q}' = \frac{8}{\pi M_0} \left[\left(\frac{1}{2} t_0^2 - \frac{1}{3} M_0 t_0^3 + \frac{1}{3} \right) \text{arc cos} \frac{M_0 t_0 - 1}{t_0} + \right.$$

$$\frac{M_0}{3\beta} \text{arc cos} (M_0 - \beta^2 t_0) + \left(\frac{2}{9} t_0^2 + \frac{1}{9} M_0^2 t_0^2 - \frac{7}{18} M_0 t_0 + \right.$$

$$\left. \left. \frac{11}{18} \right) \sqrt{t_0^2 - (1 - M_0 t_0)^2} \right] \tag{32b}$$

and for $\frac{1}{M_0-1} \leq t_0$ (third interval)

$$C_{L_q}' = 8/3\beta \tag{32c}$$

Similarly a combination of equations (29) and (31) yields, for the pitching moment about the apex, the results

for $0 \leq t_0 \leq \frac{1}{M_0+1}$ (first interval)

$$C_{m_q}' = -\frac{2}{M_0} \left[1 + t_0^2 - \frac{1}{8} t_0^4 (1 + 4M_0^2) \right] \tag{33a}$$

for $\frac{1}{M_0+1} \leq t_0 \leq \frac{1}{M_0-1}$ (second interval)

$$C_{m_q}' = -\frac{1}{\pi M_0} \left\{ \left[2(1 + t_0^2) - \frac{1}{4} t_0^4 (1 + 4M_0^2) \right] \text{arc cos} \frac{M_0 t_0 - 1}{t_0} + \right.$$

$$\frac{2M_0}{\pi\beta} \text{arc cos} (M_0 - \beta^2 t_0) +$$

$$\left. \frac{1}{12} \left[42 - 22M_0 t_0 + (2M_0^2 + 3) t_0^2 + (2M_0^2 + 13)M_0 t_0^3 \right] \sqrt{t_0^2 - (1 - M_0 t_0)^2} \right\} \tag{33b}$$

and for $\dfrac{1}{M_0-1} \leq t_0$ (third interval)

$$C_{m_q}' = -\frac{2}{\beta} \qquad\qquad (33c)$$

Numerical results for a Mach number of 2 are presented in the next section.

Discussion of Results

Figure 4 shows the variation of C_{L_α}, C_{m_α}', and the location of $x_{c.p.}$ with τ_0, the number of chord lengths traveled ($\tau_0 = V_0 t'/c_0 = M_0 t/c_0 = M_0 t_0$) for a free-stream Mach number M_0 equal to 2. The values of C_{L_α} and C_{m_α}' are in agreement with those given in references 1 and 2. For the purpose of comparison, similar curves are shown for a two-dimensional wing having a chord c_0 equal to the root chord of the triangular wing, and for the triangular wing in reversed flow. The material necessary for the calculation of the latter curves was presented in reference 6. Several interesting conclusions can be drawn from these results.

First, notice that the total indicial lift on the triangular sinking wing is the same at every instant as that on the same wing in reversed flow (both wings of course having started with the same velocity at the same time), and that the value of this lift is the same as the total indicial lift on the two-dimensional wing only at the beginning of the motion and again when the steady state has been attained (fig. 4(a)). Such a result for reversed flow is not true for the pitching moment (fig. 4(b)) and center of pressure, and it can be shown that it is true for the total lift only when the wing is a flat lifting surface with supersonic edges.[4]

Second, notice that, since all of the characteristics for the triangular wings are independent of the angle of sweep, they are valid for any unyawed triangular wing flying at a Mach number equal to 2 and having supersonic leading edges.

Third, it is apparent from figure 4(a) that the transition of the total indicial lift from its initial to its final value is less abrupt than that transition for the two-dimensional wing, and finally the movement of the center of pressure on the sinking wing of all types is seen from figure 4(c) to be small.

---

[4] R. T. Jones has shown, in an unpublished work, that the build-up of total indicial drag on symmetrical nonlifting wings is the same for all types of plan forms in forward and reversed flow.

Finally, it can be seen from equations (27a) and (27c) that the initial and final values of C_{L_α} depend on $1/M_0$ and $1/\beta$, respectively. As the Mach number M_0 is increased, therefore, the variation dies out since β and M_0 become nearly equal. The same remark applies to all the other coefficients.

Figure 5 presents the values of $C_{L_q}{}'$, $C_{m_q}{}'$, and $x_{c.p.}/c_0$ for wings pitching about the foremost extremity of their plan form (i.e., leading edge or apex). Again the results are presented in terms of chord lengths traveled τ_0 for a free-stream Mach number equal to 2.

For these wings it is apparent that the reverse-flow theorem does not apply even to total lift. The results for the triangular wing are still independent of the angle of sweep, however, and the movement of the center of pressure is again slight.

WING WITH SUBSONIC EDGES

INDICIAL LOADING FOR SINKING WING

Analysis

The six regions.— As in the study of supersonic-edged triangular wings, there are also in the case of triangular wings with subsonic leading edges various regions in which the analytical form of the loading equation is different. Figure 6 shows the regions into which the subsonic-edged triangular wing can be most conveniently divided. Most of these regions have counterparts on the supersonic-edged wing shown in figure 1.

To begin with, region 6 lies within the spherical wave which started at $t=0$ from the wing apex. Region 1 is within the cylindrical wave which was started at $t=0$ by one edge of the wing, but outside the wave started by the other edge. Region 4 is the area formed by the overlapping of the two cylindrical waves from the opposite edges, but outside the region influenced by the reflection of one of these waves on the opposite edge (secondary wave fronts shown in the figure). Region 5 is the area between regions 4 and 6 where the flow is influenced by secondary (and higher-order) wave reflections. Finally, regions 2 and 3 are similar to regions 2 and 3 in the supersonic-edged case; region 2 being that uninfluenced by the starting phenomena and therefore having a loading already at its steady-state value, and region 3 being that which is unaffected by the disturbances emanating from the edges.

Region 1: The solution for the load distribution in region 1 is the same as that for a two-dimensional wing starting suddenly from rest and moving with a steady subsonic velocity V_n. A solution to the latter problem for the initial part of the motion is presented in reference 7. In terms of the normal components of velocity and distance, therefore, the loading coefficient for the right-hand side of figure 6 can be written immediately:

$$\left(\frac{\Delta p}{q_n}\right)_1 = -\frac{8w_0}{\pi V_n M_n}\left(\frac{M_n}{1+M_n}\sqrt{\frac{t-x_n}{M_n t + x_n}} + \text{arc } \tan\sqrt{\frac{M_n t + x_n}{t-x_n}}\right)$$

The equations which relate the normal components to those in the free-stream direction have already been given in the section on region 4 of the supersonic-edged wing. Use of these relations leads to the following expression for loading in region 1 (in the coordinate system of fig. 7)

$$\left(\frac{\Delta p}{q_0}\right)_1 = \frac{8\alpha}{\pi M_0}\left(\frac{mM_0}{mM_0+\sqrt{1+m^2}}\sqrt{\frac{t\sqrt{1+m^2} + |y| - mx}{m M_0 t - |y| + mx}} + \right.$$

$$\left. \text{arc } \tan\sqrt{\frac{mM_0 t - |y| + mx}{t\sqrt{1+m^2} + |y| - mx}}\right) \qquad (34)$$

Region 2: The loading on region 2, being the steady-state loading on a triangular wing with subsonic edges, is well known. The solution for region 2 of figure 7 is therefore given by (see, for convenience, reference 5)

$$\left(\frac{\Delta p}{q_0}\right)_2 = \frac{4\alpha m^2(x+M_0 t)}{\sqrt{m^2(x+M_0 t)^2 - y^2}\ E} \qquad (35)$$

where E is the complete elliptic integral of the second kind with modulus $\sqrt{1-\beta^2 m^2}$

Region 3: The loading in region 3 follows from reference 6 and is

$$\left(\frac{\Delta p}{q_0}\right)_3 = \frac{4\alpha}{M_0} \qquad (36)$$

Region 4: The loading in region 4 of figure 7 is calculated by superposition, just as the solution for region 5 of the wing with supersonic edges was obtained. The solution in region 4 is the sum of the solutions for the right and left halves of region 1, minus the result for region 3. Thus

$$
\left(\frac{\Delta p}{q_0}\right)_4 = \frac{8\alpha}{\pi M_0}\left[\frac{mM_0}{mM_0 + \sqrt{1+m^2}}\left(\sqrt{\frac{t\sqrt{1+m^2}-y-mx}{mM_0 t+y+mx}}+\right.\right.
$$

$$
\left.\sqrt{\frac{t\sqrt{1+m^2}+y-mx}{mM_0 t-y+mx}}\right) + \text{arc } \tan\sqrt{\frac{mM_0 t+y+mx}{t\sqrt{1+m^2}-y-mx}} +
$$

$$
\text{arc } \tan\sqrt{\frac{mM_0 t - y + mx}{t\sqrt{1+m^2} + y - mx}} - \frac{\pi}{2}\Bigg] \tag{37}
$$
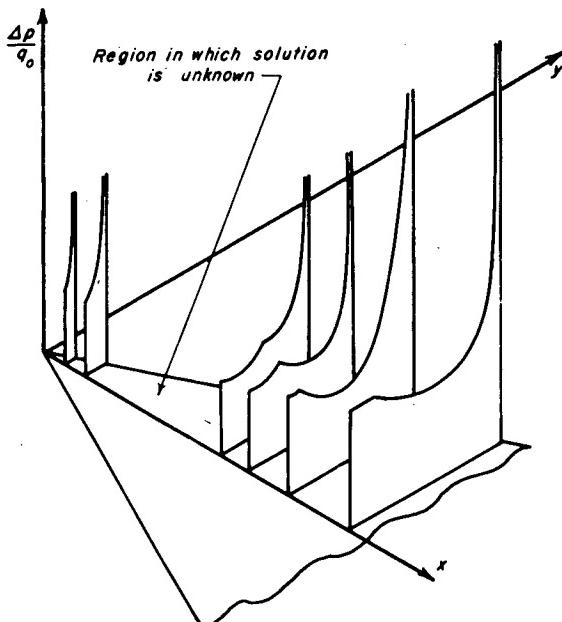
Regions 5 and 6: In these regions the exact solution for the loading has not been determined. As was shown in reference 4, such solutions would require the solution of a three-dimensional elliptic-type partial differential equation. In this report a later section will contain an approximate solution for these regions.

Discussion of Results

An isometric drawing of the load distribution, for the regions in which it is known, is shown in the sketch. Comparing the results for the loading on this wing to the one with supersonic edges (fig. 3), it is apparent that the principal difference in the two distributions is in the behavior around the leading edges; the loading being finite at the supersonic edge, whereas it becomes infinite at the subsonic edge. In view of the known steady-state results this difference was to be expected. Elsewhere the loadings are quite similar.

The results presented in equations (34) through (37) will next be examined in a different light. Choose a given spanwise section on the wing and watch this section as time progresses from t=0. This amounts to fixing the axis on the body and can be accomplished simply by using the quantity s introduced in equation (21),

$$s = m(x + M_0 t)$$

It is clear that s is the semispan of a given spanwise section, and that if equations (34) through (37) are written in terms of s, y, and t, for a fixed s they represent the variation of loading on a given section as time progresses.

If the notation is further simplified by introducing the parameter β_θ where

$$\beta_\theta = \frac{1}{mM_0 + \sqrt{1+m^2}} \qquad (38)$$

equations (34) through (37) can be written in the following way:

$$\left(\frac{\Delta p}{q_0}\right)_1 = \frac{8\alpha}{\pi M_0}\left(mM_0\beta_\theta \sqrt{\frac{t/\beta_\theta - s + |y|}{s - |y|}} + \arctan \sqrt{\frac{s - |y|}{t/\beta_\theta - s + |y|}}\;\right) \qquad (39)$$

$$\left(\frac{\Delta p}{q_0}\right)_2 = \frac{4\alpha ms}{E\sqrt{s^2 - y^2}} \qquad (40)$$

$$\left(\frac{\Delta p}{q_0}\right)_3 = \frac{4\alpha}{M_0} \qquad (41)$$

$$\left(\frac{\Delta p}{q_0}\right)_4 = \frac{8\alpha}{\pi M_0}\left(mM_0\beta_\theta \sqrt{\frac{t/\beta_\theta + y - s}{s - y}} + mM_0\beta_\theta \sqrt{\frac{t/\beta_\theta - y - s}{s + y}} + \right.$$

$$\left. \arctan \sqrt{\frac{s - y}{t/\beta_\theta + y - s}} + \arctan \sqrt{\frac{s + y}{t/\beta_\theta - y - s}} - \frac{\pi}{2}\right) \qquad (42)$$

The load distribution across any section is given by equations (39), (41), and (42) from the time $t/\beta_\theta = 0$ to $(t/\beta_\theta)_1$, where the term $(t/\beta_\theta)_1$ is equal to $2s$ or $s/m(M_0+1)\beta_\theta$, whichever is smaller.

(At $t/\beta_e = 2s$ the spanwise section has just reached the secondary waves shown in figure 6, and at $t/\beta_e = s/m\beta_e(M_0+1)$ the spanwise section has just reached the spherical wave which started from the apex.) From $(t/\beta_e)_1$ to $(t/\beta_e)_2 = s/m\beta_e(M_0-1)$, the loading has not been determined, and from $t/\beta_e = (t/\beta_e)_2$ to $t = \infty$ the loading is the steady-state value given by equation (40). The sketch shows this initial and final load variation plotted as a function of the parameter t/β_e. At the beginning of the motion the loading is constant across the span, but this type of distribution is quickly modified and the shape of the curve tends toward the "inverted elliptic" loading given by equation (40) and shown in the sketch as the distribution at $t/\beta_e = (t/\beta_e)_2$. In fact, when the span has traveled a distance such that $t/\beta_e = 2s$, the expression for the loading given by equation (42) becomes

$$\left(\frac{\Delta p}{q_0}\right)_{\frac{t}{\beta_e} = 2s} = \frac{16 \ m\beta_e s}{\pi \sqrt{s^2 - y^2}} \tag{43}$$

which differs from the value given by equation (40) only by a constant of proportionality. Both before and after the time $t/\beta_e = 2s$ the shape of the loading curve varies from the simple type represented by equation (43), but the trend, and to a certain extent the rapidity of the trend, is clearly established.

The average spanwise loading P_0, introduced by equation (20a), can now be determined for certain regions. Hence, if the notation

$$\left. \begin{array}{c} \tau = t/s \\[2ex] P_0 = \dfrac{M_0}{2s\alpha} \displaystyle\int_{-s}^{s} \dfrac{\Delta p}{q_0} \, dy \end{array} \right\} \tag{44}$$

is adopted, there results for the early part of the motion, that is, for $0 \le \tau/\beta_e \le (\tau/\beta_e)_1$

$$P_0 = 2\left(2 - \frac{\tau}{\beta_e}\right) + 4m\beta_e M_0 \ (\tau/\beta_e) \tag{45}$$
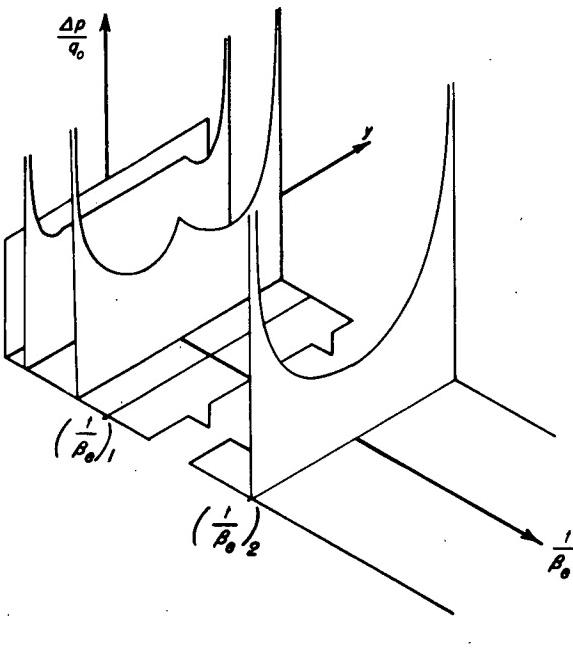
Equation (45) was derived by integrating equations (39), (41), and (42).

For values of $\tau/\beta_\Theta \geq 1/\beta_\Theta m(M_0-1) = \left(\dfrac{\tau}{\beta_\Theta}\right)_2$ equation (40) is valid.
Hence

for $\dfrac{\tau}{\beta_\Theta} \geq \left(\dfrac{\tau}{\beta_\Theta}\right)_2$

$$P_0 = \frac{2\pi m M_0}{E} \qquad\qquad (46)$$

The sketch indicates the magnitude of this average load for both large and small values of τ/β_Θ. Notice that for small values of τ/β_Θ it is sufficient for the establishment of the curve to specify the parameter $mM_0\beta_\Theta$, but for large values an additional parameter must be given (such as M_0 in the sketch). Notice, further, that in spite of the large variation in the distribution of the loading, as shown in the previous sketch, the average value P_0 varies linearly throughout the intervals considered. This result is similar to the one obtained for triangular wings with supersonic edges and is given in equations (24).
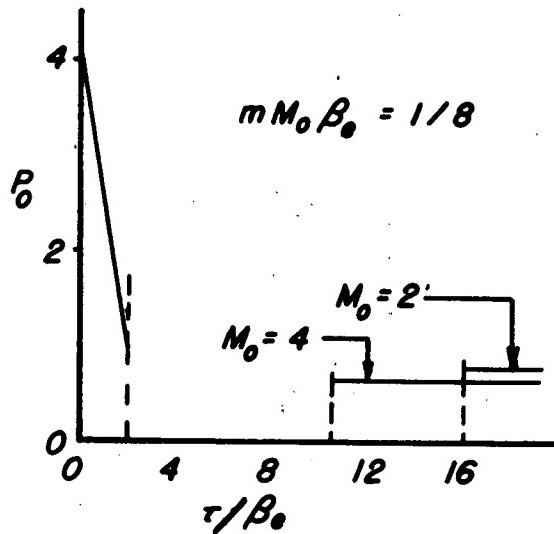
INDICIAL LOADING ON VERY SLENDER TRIANGULAR WINGS

Analysis

In the first section of this report entitled "The Problem and the Nature of its Solution," it was pointed out that if the wing is slender (i.e., has a small ratio of span to chordwise length) the basic partial differential equation (1) can be approximated by the equation which was previously introduced as equation (4), thus:

$$\varphi_{tt} - \varphi_{yy} - \varphi_{zz} = 0$$

The boundary conditions appropriate to this problem will now be examined in some detail.

Just as in the previous sections of this report, consider a triangular wing which is at rest for $t < 0$, starts suddenly to move at a forward velocity equal to V_O at $t=0$, and continues at this same velocity for $t > 0$. It should be emphasized that in this case, V_O may be either subsonic or supersonic. A section in the spanwise direction, as for instance section AA in the sketch, projects into the yt plane as a narrow rectangular strip along the t axis. Since equation (4) has been derived on the assumption that the velocity gradients in the y, z, and t directions are independent of the gradient in the x direction, the boundary conditions along the strip shown in the sketch are independent of those on other strips projected from spanwise sections along the wing. Hence, the problem is to find a solution to equation (4) which will make φ_z constant over the strip and at the same time will satisfy the other conditions listed under equation (1). In the lifting-surface analog this corresponds to the problem of finding the velocity potential over a flat rectangular wing of low aspect ratio situated in a free stream moving at a Mach number equal to $\sqrt{2}$. Solutions to the latter problem can be obtained by various techniques, and so the procedure will be first, to find the potential for the steady-state, flat, rectangular wing, and then, by analogy, to convert this to the solution for the very slender triangular wing in unsteady motion.

The steady-state, lifting-surface problem.- Lifting-surface solutions for the loading on a rectangular wing traveling at supersonic speeds have been developed for regions 1, 2, and 3 of figure 8 (by Busemann and others), and by means of these solutions the load distribution on a spanwise section of the triangular wing can be determined to a time necessary for sound to travel that span length. For $t > 2s$, however, the solution becomes considerably complicated by the increasing number of reflections from the edges. Reference 8 gives solutions for the loading on a rectangular wing in region 4 and indicates methods for extending the solution to regions farther along the wing. Already in region 4, however, the expression is cumbersome and in higher-numbered regions the expressions become difficult to manipulate. These methods, therefore, will be discarded in favor of a more approximate but simpler analysis.

If x is the distance along the chord, y the distance along the span, and s the semispan, then the solution for regions 1, 2, and 3 of
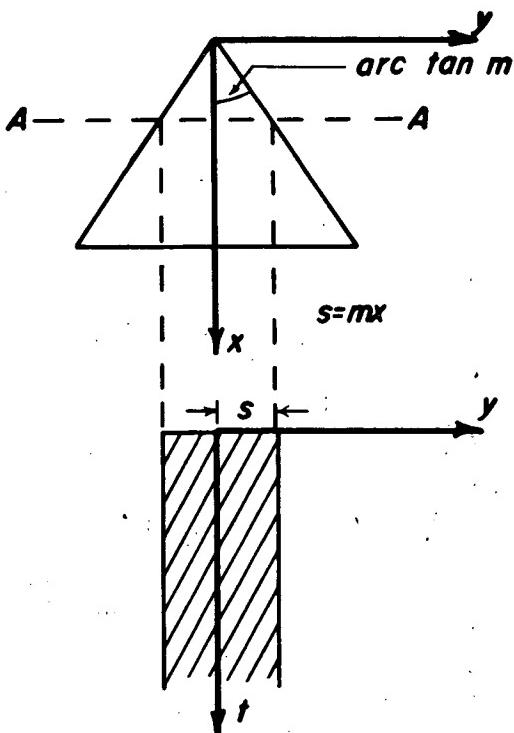
figure 8 can be written (for convenience, see reference 5):

Region 1

$$\frac{\Delta p}{q_0} = 4\alpha \tag{47a}$$

Region 2

$$\frac{\Delta p}{q_0} = \frac{8\alpha}{\pi} \text{ arc tan } \sqrt{\frac{s - |y|}{x - s + |y|}} \tag{47b}$$

Region 3

$$\frac{\Delta p}{q_0} = \frac{8\alpha}{\pi} \left(\text{arc tan } \sqrt{\frac{s+y}{x-s-y}} + \text{arc tan } \sqrt{\frac{s-y}{x-s+y}} - \frac{\pi}{2} \right) \tag{47c}$$

As x increases (i.e., for higher-numbered regions in figure 8) it is reasonable to assume that the spanwise variation of loading is relatively unimportant — except that it be "smooth" and fall to zero at the side edges — and the chordwise variation of loading is dominant. Assume, therefore, that the loading is given by the relation

$$\frac{\Delta p}{q_0} = 4\alpha \text{ f } \left(\frac{x}{s}\right) \sqrt{1 - \left(\frac{y}{s}\right)^2} \tag{48}$$
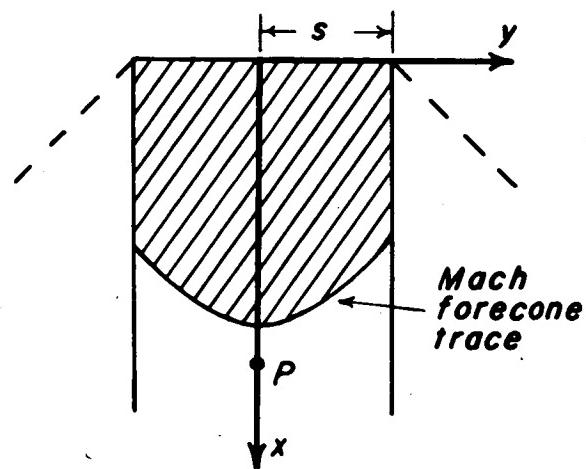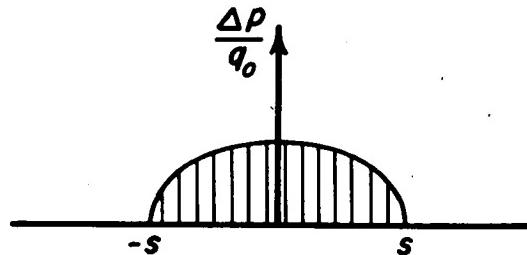
Spanwise, this has the variation shown in the preceding sketch; chord-wise it is as yet arbitrary. To fix the chordwise distribution the value of $f(x/s)$ will be determined so that the vertical induced velo-city along the center line is constant and equal to $-V_0\alpha$.

The solution to this somewhat artificial problem approaches the exact solution to the steady-state lifting-surface problem for a flat rectangular wing along sections far behind the leading edge; closer to the leading edge it only approximates the exact solution; and, of course, in the vicinity of the leading edge it will be least representative. But, on the other hand, the exact solution is known in the vicinity of the leading edge and it turns out that the solution of the problem posed above forms a reasonable continuation over the remainder of the wing.

The velocity potential for the problem which has been set can be readily expressed in terms of an integration of elementary horseshoe vortices over the plan form. Since the Mach number equals $\sqrt{2}$, then according to reference 9,

$$\varphi = \frac{V_0 z}{4\pi} \int_A \int \frac{(x-x_1)\,(\Delta p/q_0)\,dx_1 dy_1}{(y_1^2+z^2)\,\sqrt{(x-x_1)^2 - y_1^2 - z^2}}$$

where A is the area on the wing within the forecone from the point $P(x,y,z)$, at which φ is to be determined (the shaded area in the sketch).

The simplification of the last expression is given in reference 9. The result is the integral equation

$$1 = f(\eta) + \frac{2}{\pi} \int_0^\eta f(\eta_1)\, G\,(\eta-\eta_1)d\eta_1 \qquad\qquad (49)$$

where $\eta = x/s$ and G is given by

$$G(\eta-\eta_1) = \begin{cases} E_1 & 1 \le \eta-\eta_1 \\ \dfrac{E_2-(1-k_2^2)K_2}{k_2} & \\ & \eta-\eta_1 \le 1 \end{cases}$$

$$k_1 = \frac{1}{\eta-\eta_1}\;;\quad k_2 = \eta-\eta_1$$

The modulus of E_1 is k_1 and the modulus of K_2 and E_2 is k_2.

The solution of equation (49) for $f(\eta)$ is not difficult when numerical methods are used. For intervals of η_1 equal to 0.2, the result is given in tabular form in appendix A, and also in the sketch.
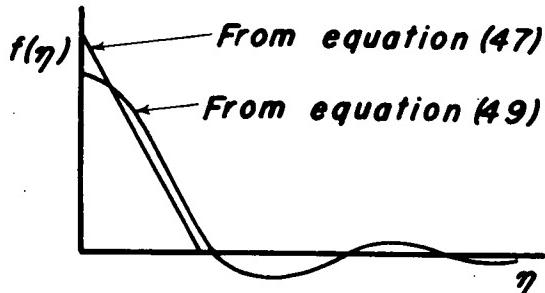
This result can be improved in the interval $0 \le \eta \le 2$ by means of the correct solution in that interval given by equations (47). Comparison of the spanwise average of the loading given by equation (48) with that which can be derived from equations (47) gives an equivalent $f(\eta)$ in the interval which, when used in equation (48), will give the correct value of the average span loading. The sketch also shows a curve for this equivalent $f(\eta)$ which starts at $4/\pi$ and falls linearly to zero at $\eta=2$.

By using the sketch, or the results listed in appendix A, the loading over a low–aspect–ratio rectangular wing flying at a Mach number equal to $\sqrt{2}$ can be estimated. Of particular interest is the damped, oscillatory nature of the load, falling to zero at one span length behind the leading edge and taking alternately negative and positive values beyond this point.[5] A somewhat different approach to this problem (reference 11) has recently led to a solution very like the one given here.

The unsteady analog, sinking wing.— The first step in deriving the unsteady–flow results for the sinking wing from the steady solution is to replace x with t. In equation (49) this corresponds to replacing η with τ where τ is equal to t/s (equation (44). The second step is to rederive the expression for loading coefficient since in the time-varying problem it is expressed in a somewhat different manner than in the steady–state analog. In the unsteady case, as the triangular wing moves through a fixed reference plane the local span intersecting

---

[5] A discussion of this aspect of these results is contained in reference 10.

this plane grows as a function of time and equation (2), which represents the partial derivative with respect to time with x fixed, must be expanded to the form

$$\frac{\Delta p}{q_o} = \frac{2}{V_o M_o} \left[\frac{\partial \Delta \varphi}{\partial t}\right]_x = \frac{2}{V_o M_o} \left(\left[\frac{\partial \Delta \varphi}{\partial t}\right]_s + \left[\frac{\partial \Delta \varphi}{\partial s}\right]_t \frac{\partial s}{\partial t}\right)$$

where $\left[\dfrac{\partial \Delta \varphi}{\partial t}\right]_s$ and $\left[\dfrac{\partial \Delta \varphi}{\partial s}\right]_t$ indicate derivatives taken at constant s and t, respectively. Since s is equal to $m(x + M_o t)$, $\partial s/\partial t$ equals $m M_o$, and there results

$$\frac{\Delta p}{q_o} = \frac{2}{V_o M_o} \left(\left[\frac{\partial \Delta \varphi}{\partial t}\right]_s + m M_o \left[\frac{\partial \Delta \varphi}{\partial s}\right]_t\right) \tag{50}$$

In the steady-state problems an analog to the term involving $\left[\dfrac{\partial \Delta \varphi}{\partial s}\right]_t$ is missing, and the loading coefficient is given entirely by an operation equivalent to $\left[\dfrac{\partial \Delta \varphi}{\partial t}\right]_s$. It is necessary, therefore, to operate further on the solution given for the loading in the steady-state problem to obtain the solution for the loading in the unsteady problem. But

$$\left[\frac{\partial \Delta \varphi}{\partial s}\right]_t = \frac{\partial}{\partial s} \int_0^t \left[\frac{\partial \Delta \varphi}{\partial t}\right]_s dt_1$$

so that if the notation

$$\left[\frac{\partial \Delta \varphi}{\partial t}\right]_s = \frac{V_o}{2} \left(\frac{\Delta p}{q_o}\right)_s$$

is adopted (where $\left(\dfrac{\Delta p}{q_o}\right)_s$ represents the loading in the analogous steady-state problem), then the expression for the unsteady loading can be given in terms of $\left(\dfrac{\Delta p}{q_o}\right)_s$ by the equation

$$\frac{\Delta p}{q_o} = \frac{1}{M_o} \left[\left(\frac{\Delta p}{q_o}\right)_s + m M_o \frac{\partial}{\partial s} \int_0^t \left(\frac{\Delta p}{q_o}\right)_s dt_1\right] \tag{51}$$

By the application of equation (51) to equations (47), the loading for the various regions of the unsteady wing can be found. For region 2 there results

$$\frac{\Delta p}{q_o} = \frac{1}{M_o}\left[\frac{8\alpha}{\pi}\arctan\sqrt{\frac{s-|y|}{t-s+|y|}} + mM_o\frac{\partial}{\partial s}\left(\int_o^{s-|y|} 4\alpha\, dt_1 + \right.\right.$$

$$\left.\left.\int_{s-|y|}^t \frac{8\alpha}{\pi}\arctan\sqrt{\frac{s-|y|}{t_1-s+|y|}}\, dt_1\right)\right]$$

which becomes

$$\frac{\Delta p}{q_o} = \frac{8\alpha}{\pi M_o}\left[mM_o\sqrt{\frac{t-s+|y|}{s-|y|}} + \arctan\sqrt{\frac{s-|y|}{t-s+|y|}}\right]$$

The loading coefficient can be similarly derived in the other regions so that finally

Region 1

$$\frac{\Delta p}{q_o} = \frac{4\alpha}{M_o} \tag{52a}$$

Region 2

$$\frac{\Delta p}{q_o} = \frac{8\alpha}{\pi M_o}\left(mM_o\sqrt{\frac{t-s+|y|}{s-|y|}} + \arctan\sqrt{\frac{s-|y|}{t-s+|y|}}\right) \tag{52b}$$

Region 3

$$\frac{\Delta p}{q_o} = \frac{8\alpha}{\pi M_o}\left(mM_o\sqrt{\frac{t-s+y}{s-y}} + mM_o\sqrt{\frac{t-s-y}{s+y}} + \right.$$

$$\left. \arctan\sqrt{\frac{s-y}{t-s+y}} + \arctan\sqrt{\frac{s+y}{t-s-y}} - \frac{\pi}{2}\right) \tag{52c}$$

For the interval $t \geq 2s$ equation (48) must be considered. By means of equation (51), the expression for the loading coefficient can be written

$$\frac{\Delta p}{q_o} = \frac{1}{M_o} \left[4\alpha \ f(\tau) \sqrt{1-\left(\frac{y}{s}\right)^2} + mM_o \frac{\partial}{\partial s} \int_0^t 4\alpha \ f\left(\frac{t_1}{s}\right) \sqrt{1-\left(\frac{y}{s}\right)^2} \ dt_1 \right]$$

which becomes

$$\frac{\Delta p}{q_o} = \frac{4\alpha}{M_o} \left[(1-mM_o\tau) \sqrt{1-\left(\frac{y}{s}\right)^2} \ f(\tau) + \frac{mM_o}{\sqrt{1-\left(\frac{y}{s}\right)^2}} \int_0^\tau f(\tau_1) d\tau_1 \right] \qquad (53)$$

where $f(\tau)$ is the solution to equation (49). Notice that for large τ (when the loading has reached its steady state), $f(\tau)$ is zero and $\int_0^\tau f(\tau_1) d\tau_1$ is unity. (See appendix A.) Hence, the loading is given by the equation

$$\frac{\Delta p}{q_o} = \frac{4\alpha m s}{\sqrt{s^2-y^2}}$$

which is the steady-state value for a slender triangular wing (equation (40) when $E = 1$).

It is now possible to derive the average span loading P_o as defined by equation (20a), thus

$$P_o = \frac{M_o}{2s\alpha} \int_{-s}^s \frac{\Delta p}{q_o} \ dy$$

Placing equations (52) and (53) in this expression, it is found that for $0 \leq \tau \leq 2$

$$P_o = 2(2-\tau) + 4mM_o\tau \qquad (54a)$$

and for $\tau \geq 2$

$$P_o = \pi(1-mM_o\tau)f(\tau) + 2 \ mM_o\pi \int_0^\tau f(\tau_1) \ d\tau_1 \qquad (54b)$$

Since the values of P_o given by equations (54a) and (54b) were derived using different methods, their magnitudes at $\tau = 2$ are not

equal. The final curve for P_0 must be constructed by fairing the solu-
tion for $\tau \leq 2$ into that for $\tau > 2$. The accompanying sketch shows
these results together with the final curve chosen (solid line).
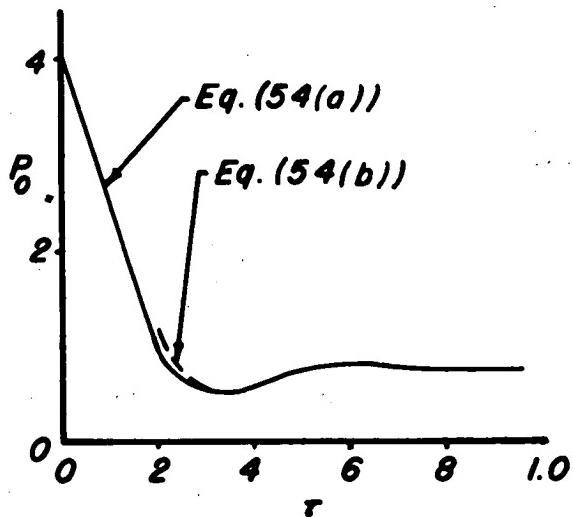
The unsteady analog, pitching wing.— When the wing is pitching at a
steady rate about its apex, the equation for the vertical induced veloc-
ity on the plan form is

$$w_u = -(x + M_0 t)\dot{\theta}$$

so that the α in the steady—state equations (47) and (48) must be
replaced by $\dot{\theta}s/mV_0$. Since the loading coefficient is still given by
equation (51), there results for the conversion of equation (48) the
expression

$$\frac{\Delta p}{q_0} = \frac{4\dot{\theta}}{mM_0V_0}\left[\sqrt{s^2-y^2}\ f(\tau) + mM_0\ \frac{\partial}{\partial s}\ s\sqrt{s^2-y^2}\int_0^{t/s} f(\tau_1)\ d\tau_1\right]$$

and this can be reduced to the form

$$\frac{\Delta p}{q_0} = \frac{4\dot{\theta}}{mM_0V_0} \ (1-mM_0\tau) \ \sqrt{s^2-y^2} \ f(\tau) \ +$$

$$\frac{4\dot{\theta}}{V_0} \ \left(\frac{2s^2-y^2}{\sqrt{s^2-y^2}}\right)\int_0^\tau \ f(\tau_1) \ d\tau_1 \tag{55}$$

As in the discussion of equation (53), it can be seen that equation (55) becomes for the steady state (τ large)

$$\frac{\Delta p}{q_0} = \frac{4\dot{\theta}}{V_0} \ \left(\frac{2s^2-y^2}{\sqrt{s^2-y^2}}\right)$$

and this can be shown to agree with the steady-state slender-wing results given in reference 12.

It is now possible to derive the average span loading P_1 as defined by equation (20b)

$$P_1 = \frac{mM_0V_0}{2s^2\dot{\theta}} \int_{-s}^{s} \frac{\Delta p}{q_0} \ dy$$

Using equation (55), one finds for $\tau > 2$

$$P_1 = \pi(1-mM_0\tau) \ f(\tau) \ + \ 3mM_0\pi \int_0^\tau \ f(\tau_1) \ d\tau_1 \tag{56a}$$

and a similar analysis based on equation (47) yields

for $0 \leq \tau \leq 2$

$$P_1 = \frac{2s}{m} \ (2-\tau+4mM_0\tau-\frac{1}{2} \ mM_0\tau^2) \tag{56b}$$

As in the case for P_0, the two equations for P_1 do not join at $\tau=2$ and the final curve must be constructed by fairing the solution for $\tau \leq 2$ into that for $\tau \geq 2$.

Discussion of Results

It is now possible to
assess the accuracy of the
solution for very slender
wings in the interval $0 \leq \tau \leq 2$
by comparing equations (52)
and (54a) with equations (41),
(39), (42), and (45), the
exact solutions for this region
derived in the preceding sec-
tion. It is apparent that the
approximate solution differs
from the exact only by a
stretching factor in the t
direction. Hence, if τ is
replaced by τ / β_e and m
(note m is proportional to
y/t) by $m\beta_e$, where β_e is
given by equation (38), then
equations (52a), (b), and (c)
are identical with equa-
tions (41), (39), and (42), respectively, and, of course, equation (54a)
corresponds to equation (45).
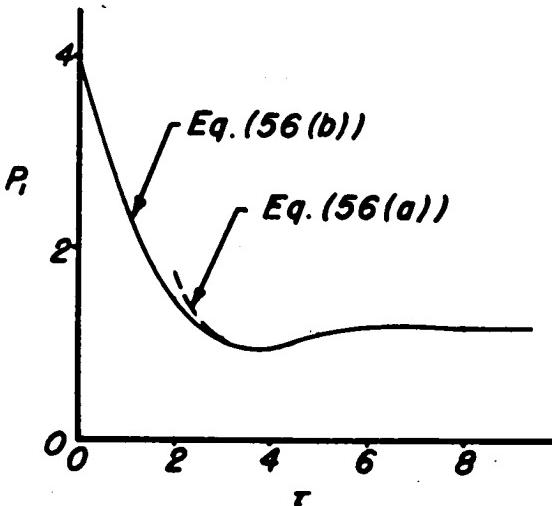
This rather remarkable result can be enlarged upon from another
viewpoint. Suppose that in the steady-state analog problem the wing had
been flying at some Mach number other than $\sqrt{2}$, say M_e. The solution
to such a new problem could be obtained from the old one merely by
applying the Prandtl-Glauert correction, that is, by stretching all dis-
tances in the x direction by the factor $1/\beta_e$ where $\beta_e^2 = |1-M_e^2|$.
Such a procedure would convert, for example, equation (54a) to the form

$$P_0 \beta_e = 2(2 - \tau / \beta_e) + 4m\beta_e M_0 \ \tau / \beta_e$$

Finally, if P_0 is adjusted so that $P_0 = 4$ at $\tau = 0$, there results

$$P_0 = 2(2 - \tau / \beta_e) + 4mM_0 \tau$$

which is exactly the answer given by equation (45). It is possible to
simplify the statement of this procedure by simply remarking: The exact
results for $\Delta p/q_0$ or P_0 in the interval $0 \leq \tau / \beta_e \leq 2$ can be
obtained from the approximate results for a very slender wing by making
an effective Mach number correction to the right-hand side of equa-
tions (52) or (54a), respectively.

It is interesting to pursue this concept even further. Consider a spanwise section of a triangular wing as time increases from the starting impulse. The primary wave fronts emanating from either side pass across the section forming the Mach lines in the steady—state rectangular—wing analogy. For very slender wings these lines make a $45°$ angle with the trace of the side edge and are used to divide the plan form into regions as in the sketch. Now find the actual position of these primary wave fronts as they form a trace on the section in the $y\tau$ plane. A straight—forward calculation shows that these lines actually make an angle equal to arc tan $1/\beta_\Theta$ with the trace of the side edges. Hence the effective Mach number which is used to correct the slender—wing results in the interval $0 \leq \tau \leq 2\beta_\Theta$ is that which makes the Mach lines of the steady-state analogy coincide with the actual trace of the primary wave fronts.
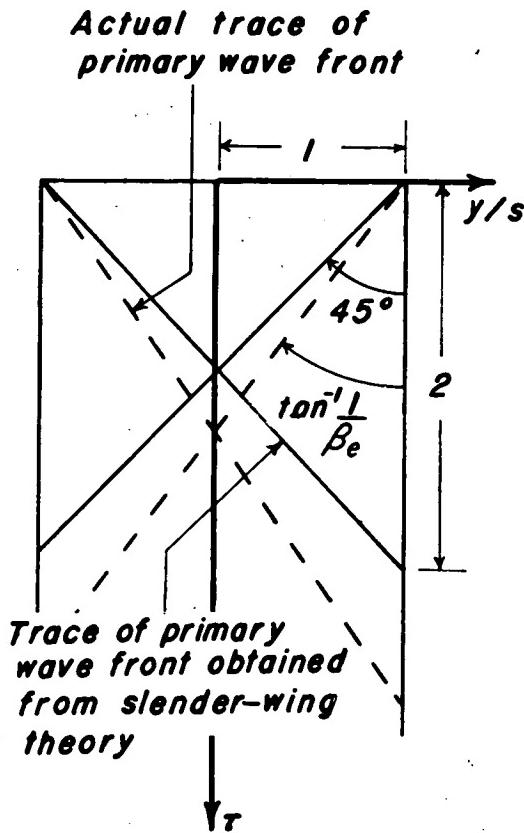
Actual trace of primary wave front

$45°$

$\tan^{-1}\dfrac{l}{\beta_e}$

Trace of primary wave front obtained from slender-wing theory

INDICIAL LIFT AND PITCHING MOMENT ON
VERY SLENDER TRIANGULAR WINGS

Analysis

The lift coefficient for the sinking wing is given in the notation introduced in equation (21a) by the equation

$$C_L = \frac{\alpha}{mc_o^2} \int_0^{c_0} \frac{2s}{M_0} P_0 dx$$

where P_O has been determined in the last section as a function of $\tau = t/s$. Consider the situation at a certain fixed time and let the x coordinate in the above formula be fixed in the wing. Then set

$$\zeta = \frac{x}{c_O} = \frac{s}{mc_O}. \tag{57}$$

and as before

$$\tau_O = \frac{M_O t}{c_O} = mM_O \zeta\tau \tag{58}$$

where τ_O is the number of wing–chord lengths traveled. In this way the equation for lift coefficient becomes

$$M_O C_{L_\alpha} = 2 \int_0^1 \zeta \, P_O \left(\frac{\tau_O}{mM_O \zeta} \right) \, d\zeta \tag{59}$$

and by a similar analysis the pitching–moment coefficient taken about the apex can be written

$$M_O C_{m_\alpha}{}' = -2 \int_0^1 \zeta^2 \, P_O \left(\frac{\tau_O}{mM_O \zeta} \right) \, d\zeta \tag{60}$$

The equation for the lift and pitching–moment coefficients (where again the pitching moment is taken about the apex) on a pitching wing are

$$M_O C_{L_q}{}' = \frac{M_O C_L}{\left(\frac{c_O \dot\theta}{V_O} \right)} = 2 \int_0^1 \zeta^2 \, P_1 \left(\frac{\tau_O}{mM_O \zeta} \right) \, d\zeta \tag{61}$$

and

$$M_O C_{m_q}{}' = \frac{M_O C_m}{\left(\frac{c_O \dot\theta}{V_O} \right)} = -2 \int_0^1 \zeta^3 \, P_1 \left(\frac{\tau_O}{mM_O \zeta} \right) \, d\zeta \tag{62}$$

Discussion of Results

The values of P_O and P_1 were taken from curves similar to the sketches in the last section (using the faired curves in the vicinity of $\tau = 2$) and the results for the indicial lift and pitching moment in terms of τ_O, the number of chord lengths traveled, are shown in figures (9) and (10) for a value of mM_O equal to 1/8. The results are all

qualitatively alike; in each case the curve falls from its high initial value at $\tau_0=0$ to a minimum at about $\tau_0=1/3$ and then recovers and practically attains its asymptotic value at $\tau_0=1$. This behavior is similar to that for a two-dimensional wing flying at subsonic speeds. For the purpose of such a comparison the first part of the curve of indicial lift coefficient versus chord lengths traveled on a two-dimensional wing flying at a Mach number equal to 0.8 (see reference 7) is shown in the sketch. Notice again the rapid fall from the initial peak $(C_{L_\alpha}=4/M_0)$ to a minimum around $\tau_0=1/2$, and then a smooth recovery to the asymptotic value $(C_{L_\alpha}=2\pi/\beta)$.
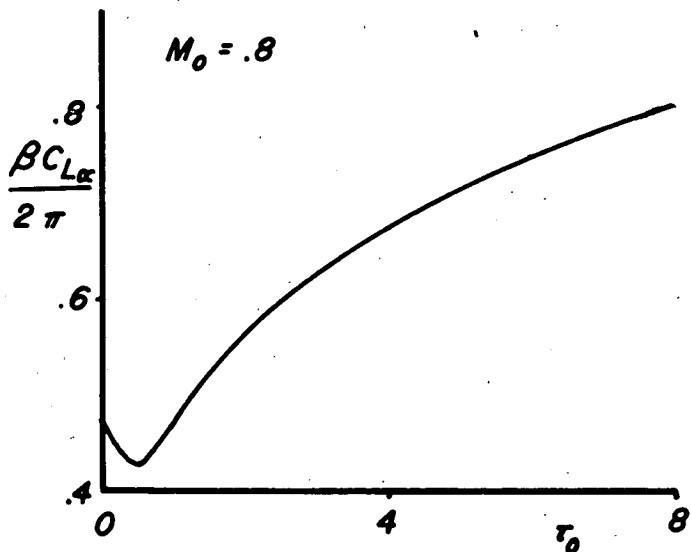
$$\frac{\beta C_{L_\alpha}}{2\pi} \qquad M_0 = .8$$

Ames Aeronautical Laboratory,
      National Advisory Committee for Aeronautics,
            Moffett Field, Calif., Mar. 26, 1951.

APPENDIX A

SOLUTION OF AN INTEGRAL EQUATION

For convenience in applying equations (54b) and (56a) of the text, a table of values of the function $f(\eta)$, obtained by numerical solution of equation (49), is given here. The values of the integral, $\int_0^\eta f(\eta_1)d\eta_1$, are also listed.

η	$f(\eta)$	$\int_0^\eta f(\eta_1)d\eta_1$	η	$f(\eta)$	$\int_0^\eta f(\eta_1)d\eta_1$
0.0	1.0000	0.0000	4.0	-0.1307	1.0124
.2	.9899	.1990	4.2	-.1008	.9893
.4	.9597	.3940	4.4	-.0716	.9720
.6	.9087	.5808	4.6	-.0446	.9604
.8	.8356	.7552	4.8	-.0207	.9539
1.0	.7339	.9122	5.0	-.0008	.9517
1.2	.6032	1.0459	5.2	.0149	.9531
1.4	.4597	1.1522	5.4	.0265	.9573
1.6	.3188	1.2300	5.6	.0340	.9633
1.8	.1880	1.2807	5.8	.0379	.9705
2.0	.0724	1.3067	6.0	.0388	.9782
2.2	-.0245	1.3115	6.2	.0373	.9858
2.4	-.1008	1.2990	6.4	.0338	.9929
2.6	-.1562	1.2733	6.6	.0292	.9992
2.8	-.1919	1.2385	6.8	.0237	1.0045
3.0	-.2098	1.1983	7.0	.0180	1.0087
3.2	-.2126	1.1561	7.2	.0124	1.0117
3.4	-.2031	1.1145	7.4	.0072	1.0137
3.6	-.1843	1.0758	7.6	.0026	1.0146
3.8	-.1593	1.0414	7.8	-.0012	1.0148

REFERENCES

1. Strang, W. J.: Transient Lift of Three-Dimensional Purely Supersonic
     Wing. Proc. Roy. Soc., Series A, June 22, 1950, pp. 54-80.

2. Miles, John W.: Transient Loading of Wide Delta Airfoils at Super-
     sonic Speeds. Navord Rep. 1235, 1950.

3. Miles, John W.: On Harmonic Motion of Wide Delta Airfoils at Super-
     sonic Speeds. Navord Rep. 1234, 1950.

4. Lomax, Harvard, Heaslet, Max. A., and Fuller, Franklyn B.: Three-
     Dimensional, Unsteady Lift Problems in High-Speed Flight - Basic
     Concepts. NACA TN 2256, 1950.

5. Jones, Arthur L., and Alksne, Alberta: The Load Distribution Due to
     Sideslip on Triangular, Trapezoidal, and Related Plan Forms in
     Supersonic Flow. NACA TN 2007, 1950.

6. Heaslet, Max. A., and Lomax, Harvard: Two-Dimensional Unsteady Lift
     Problems in Supersonic Flight. NACA Rep. 945, 1949.

7. Heaslet, Max. A., Lomax, Harvard, and Spreiter, John R.: Linearized
     Compressible-Flow Theory for Sonic Flight Speeds. NACA Rep. 956,
     1950. (Formerly TN 1824)

8. Lagerstrom, P. A., and Graham, Martha E.: Low Aspect Ratio Rectan-
     gular Wings in Supersonic Flow. Douglas Aircraft Company, Inc.
     Rep. No. SM 13110, Dec. 1947.

9. Lomax, Harvard, Heaslet, Max. A., and Fuller, Franklyn B.: Formulas
     for Source, Doublet, and Vortex Distributions in Supersonic Wing
     Theory. NACA TN 2252, 1950.

10. Lomax, Harvard, and Sluder, Loma: Chordwise and Compressibility
      Corrections to Slender-Wing Theory. NACA TN 2295, 1951.

11. Stewartson, K.: Supersonic Flow Over an Inclined Wing of Zero
      Aspect Ratio. Proc. Cambridge Phil. Soc., vol. 46, pt. 2,
      April 1950, pp. 307-315.

12. Ribner, Herbert S.: The Stability Derivatives of Low-Aspect-Ratio
      Triangular Wings at Subsonic and Supersonic Speeds. NACA TN 1423,
      1947.
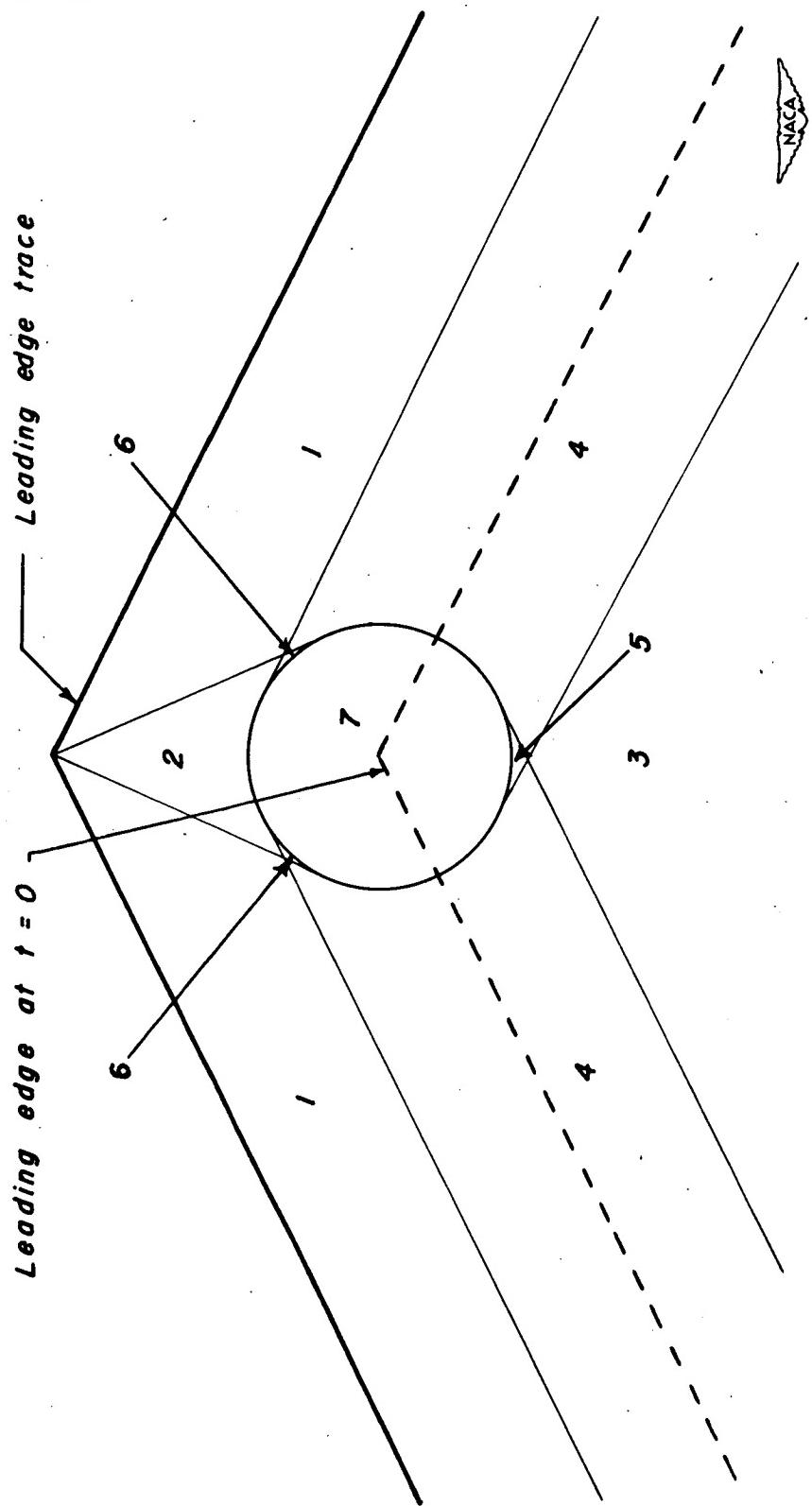
Figure 1.- The seven regions used in the analysis of the triangular wing with supersonic leading edges.

$y = -m(x + M_0 t)$

$y = -(x + M_0 t)/\beta$

$x^2 + y^2 = t^2$

$m = ctn \Delta$

$\beta = \sqrt{M_0^2 - 1}$

$y = m(x + M_0 t)$

$M_0 t$

Δ

$y = m\left(x - \dfrac{t\sqrt{1 + m^2}}{m}\right)$

$y = m\left(x + \dfrac{t\sqrt{1 + m^2}}{m}\right)$

$y = -m\left(x - \dfrac{t\sqrt{1 + m^2}}{m}\right)$
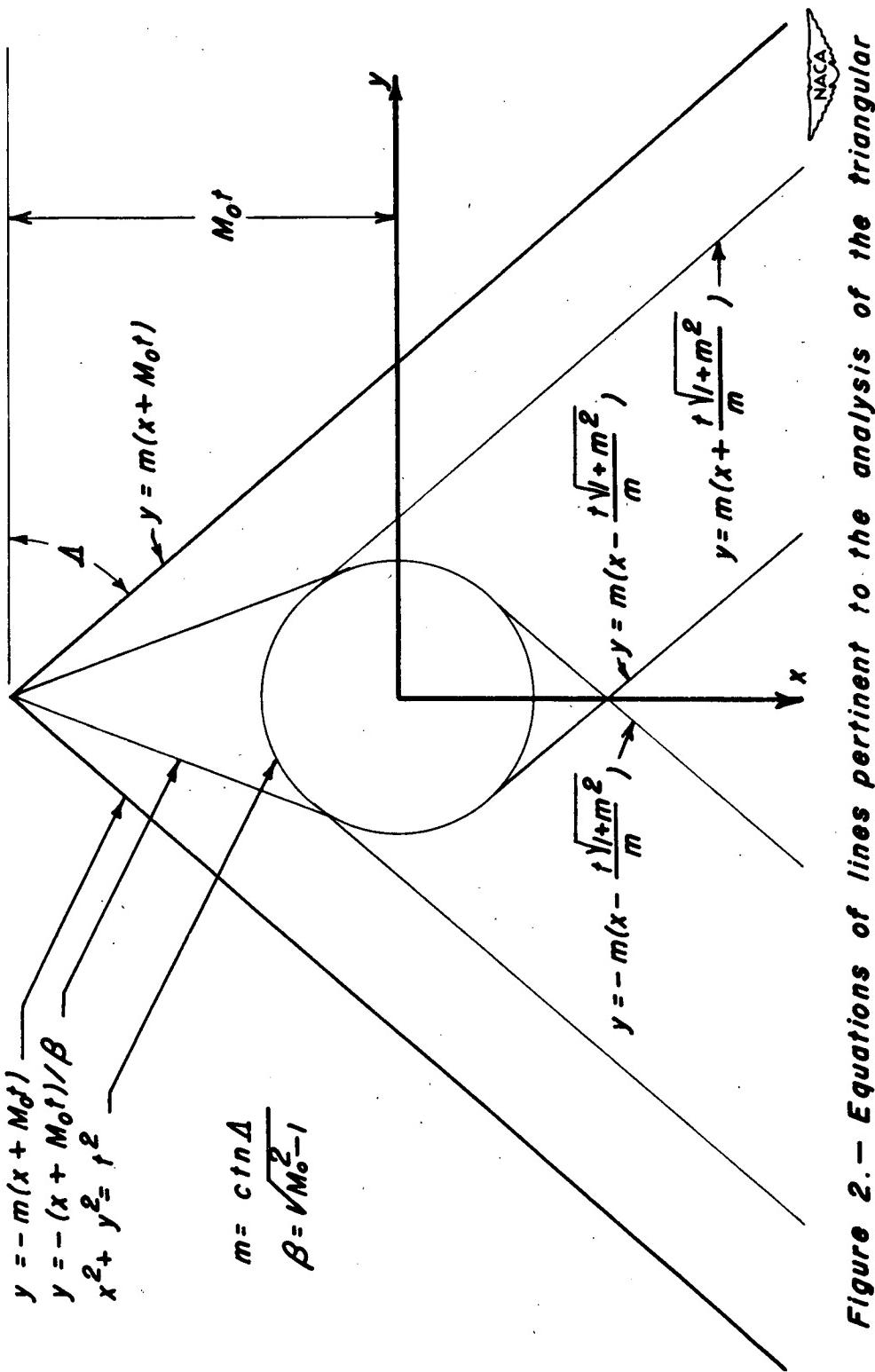
Figure 2.— Equations of lines pertinent to the analysis of the triangular wing with supersonic leading edges.
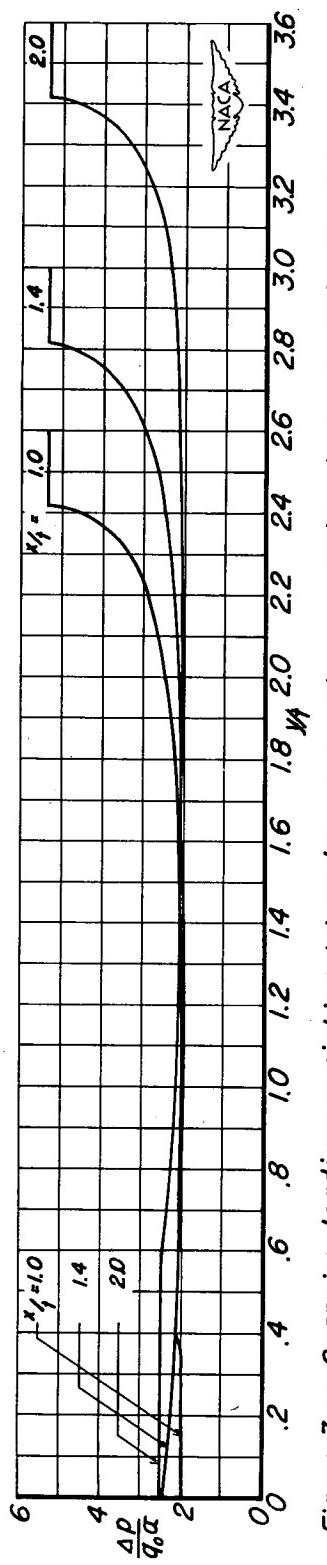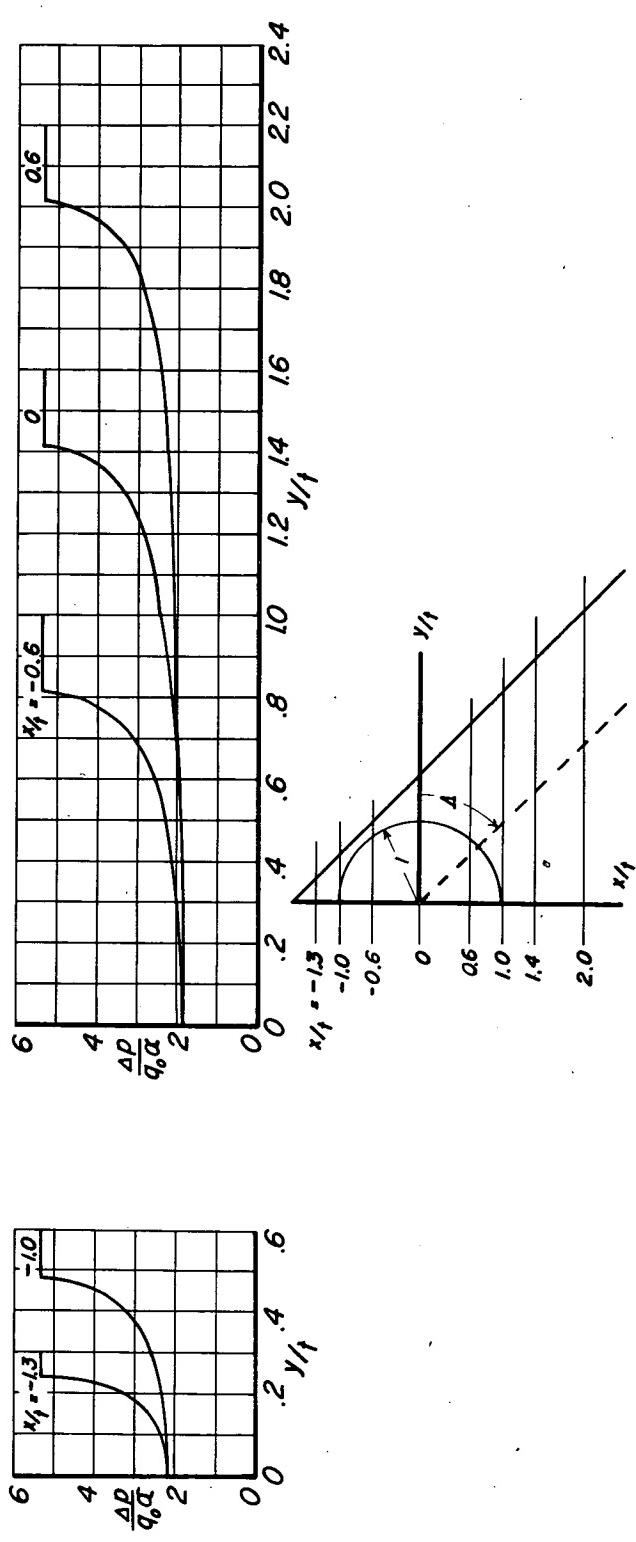
Figure 3.- Spanwise loading on sinking triangular wing with supersonic edges, Λ = 45°, M₀ = 1.6.

(a) Lift.
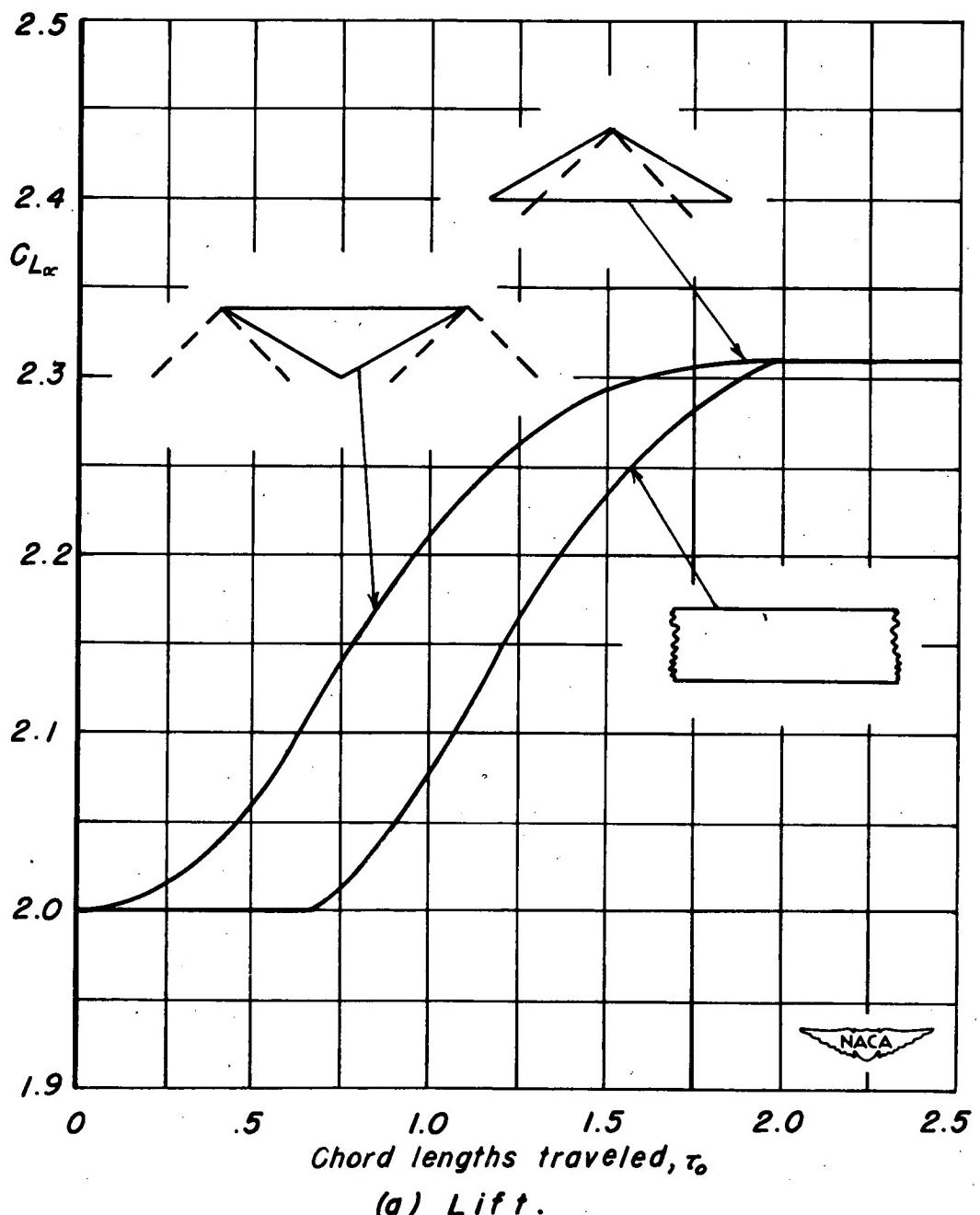
Figure 4.— Indicial aerodynamic characteristics of sinking wings with supersonic leading edges. $M_0 = 2$.
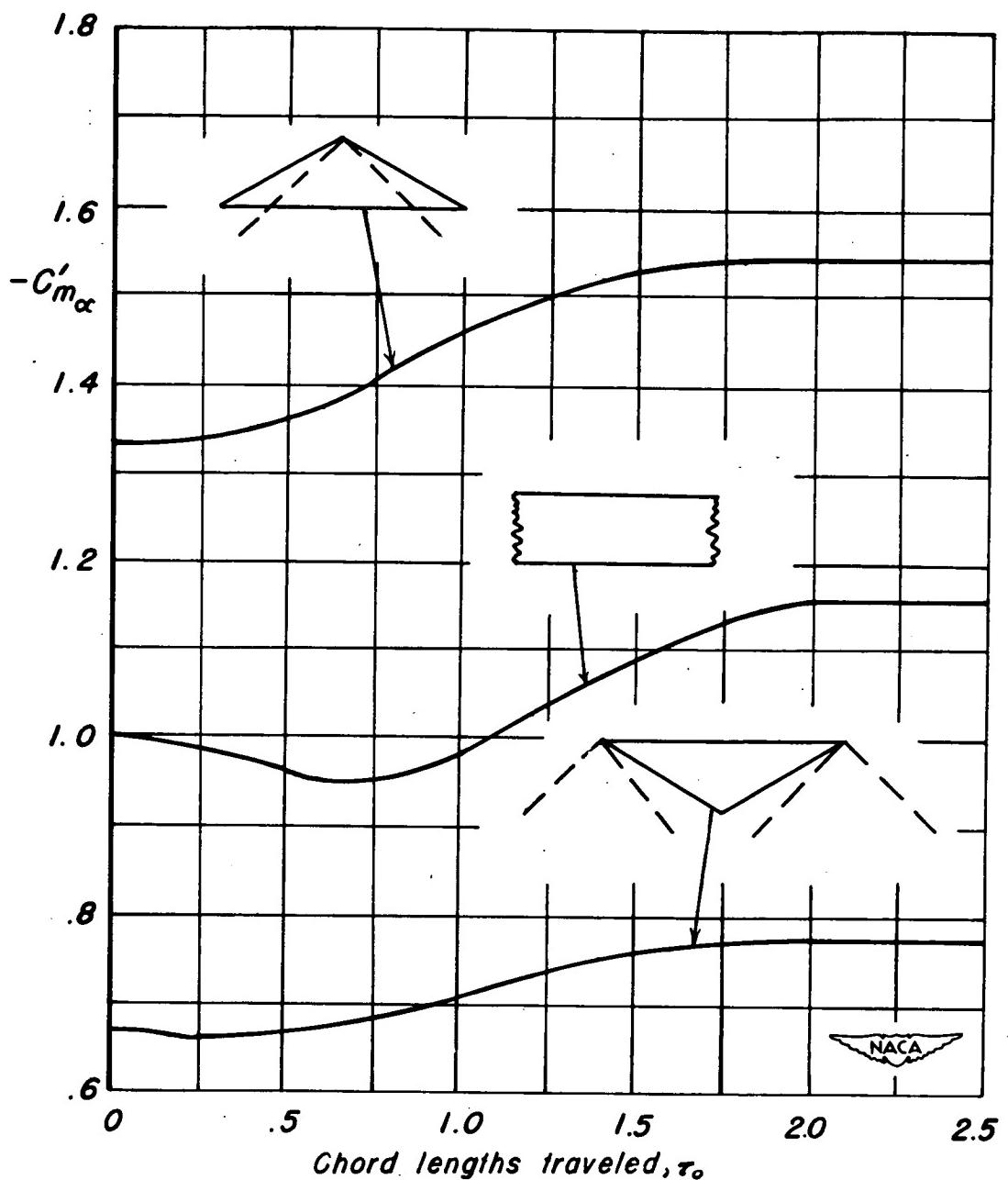
(b) Pitching moment about
    leading edge or apex.

Figure 4. — Continued.
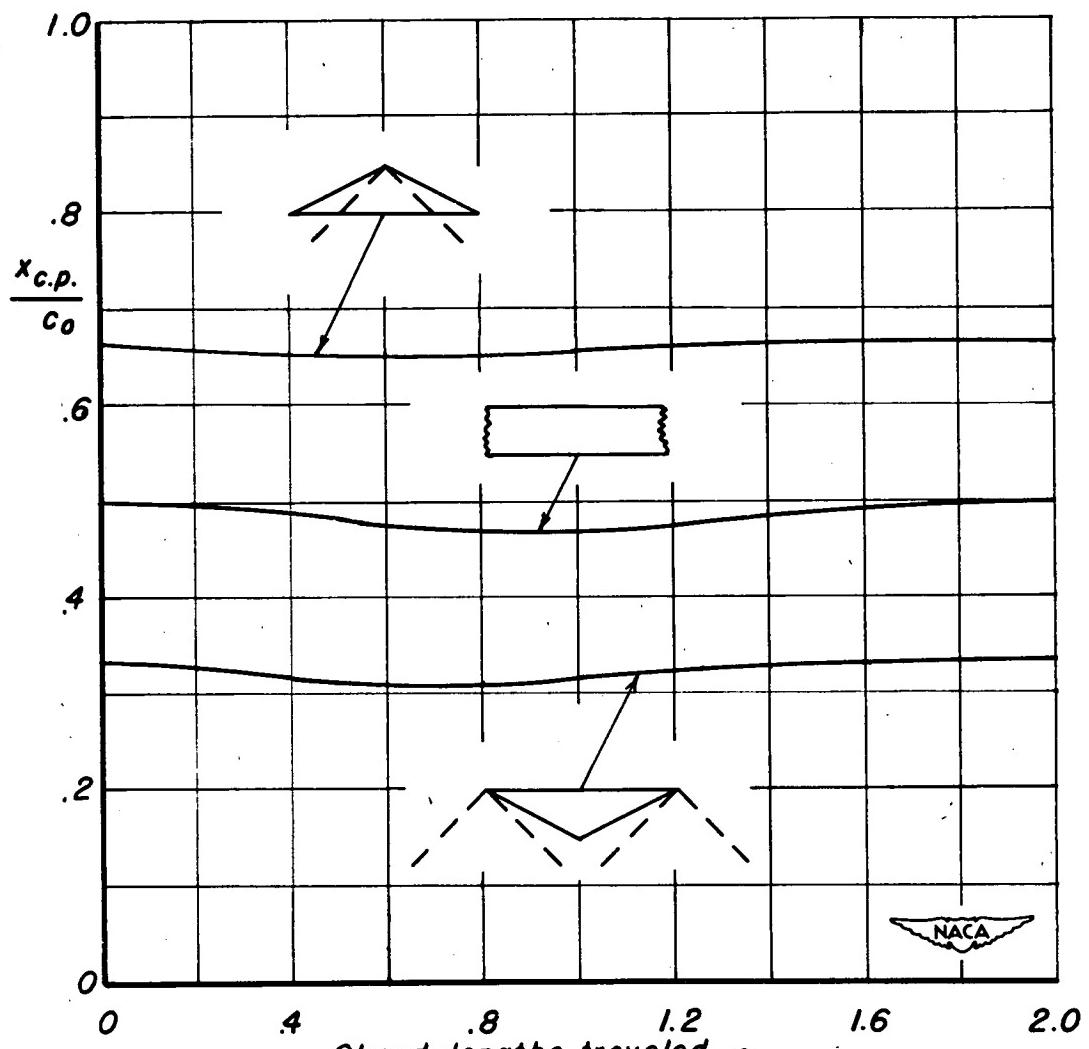
(c) Location of center of pressure
with reference to the leading
edge or apex.

Figure 4.— Concluded.
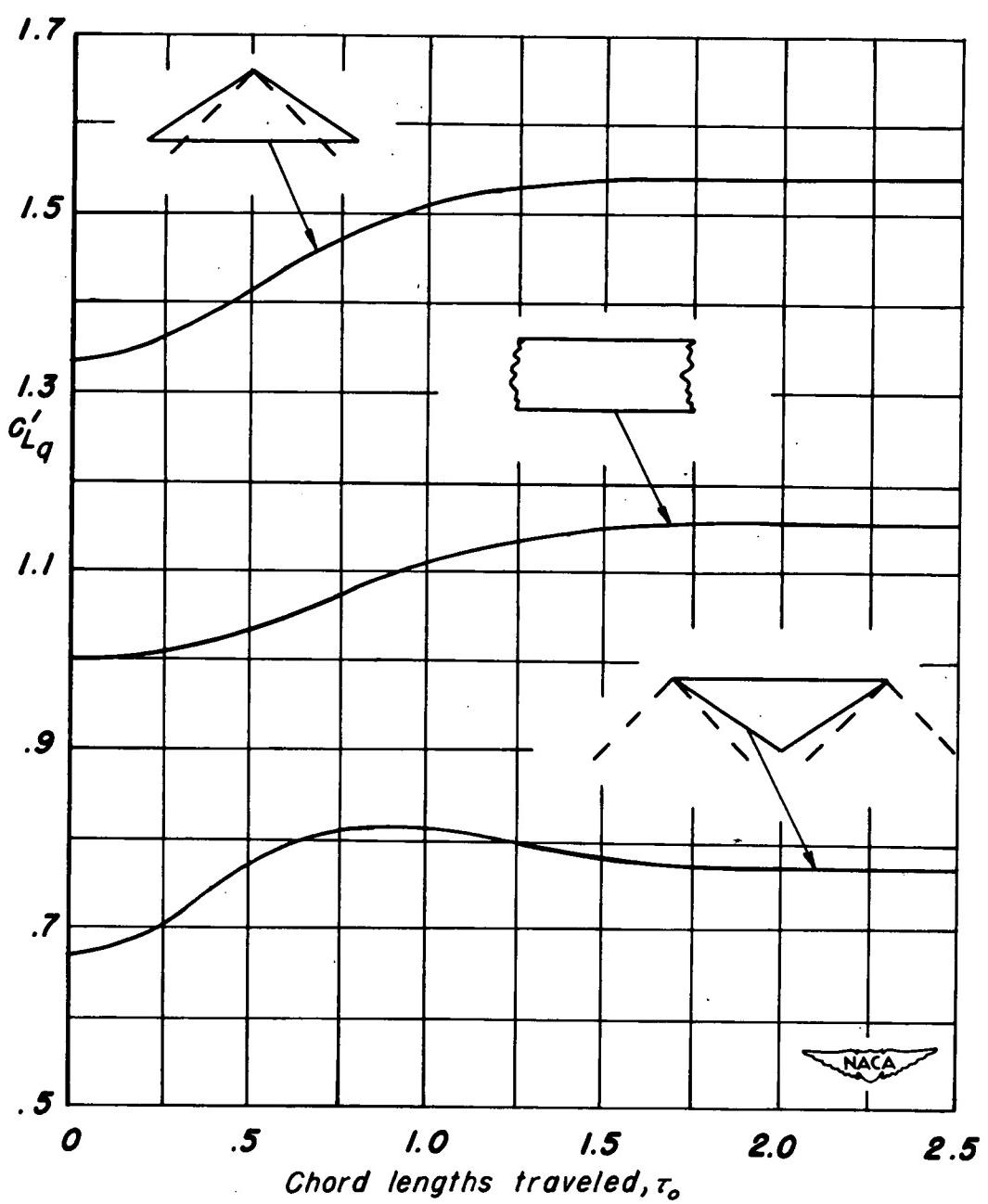
(a) Lift.

Figure 5.— Indicial aerodynamic characteristics of
wings with supersonic edges pitching about lead-
ing edge or apex. $M_o = 2$.
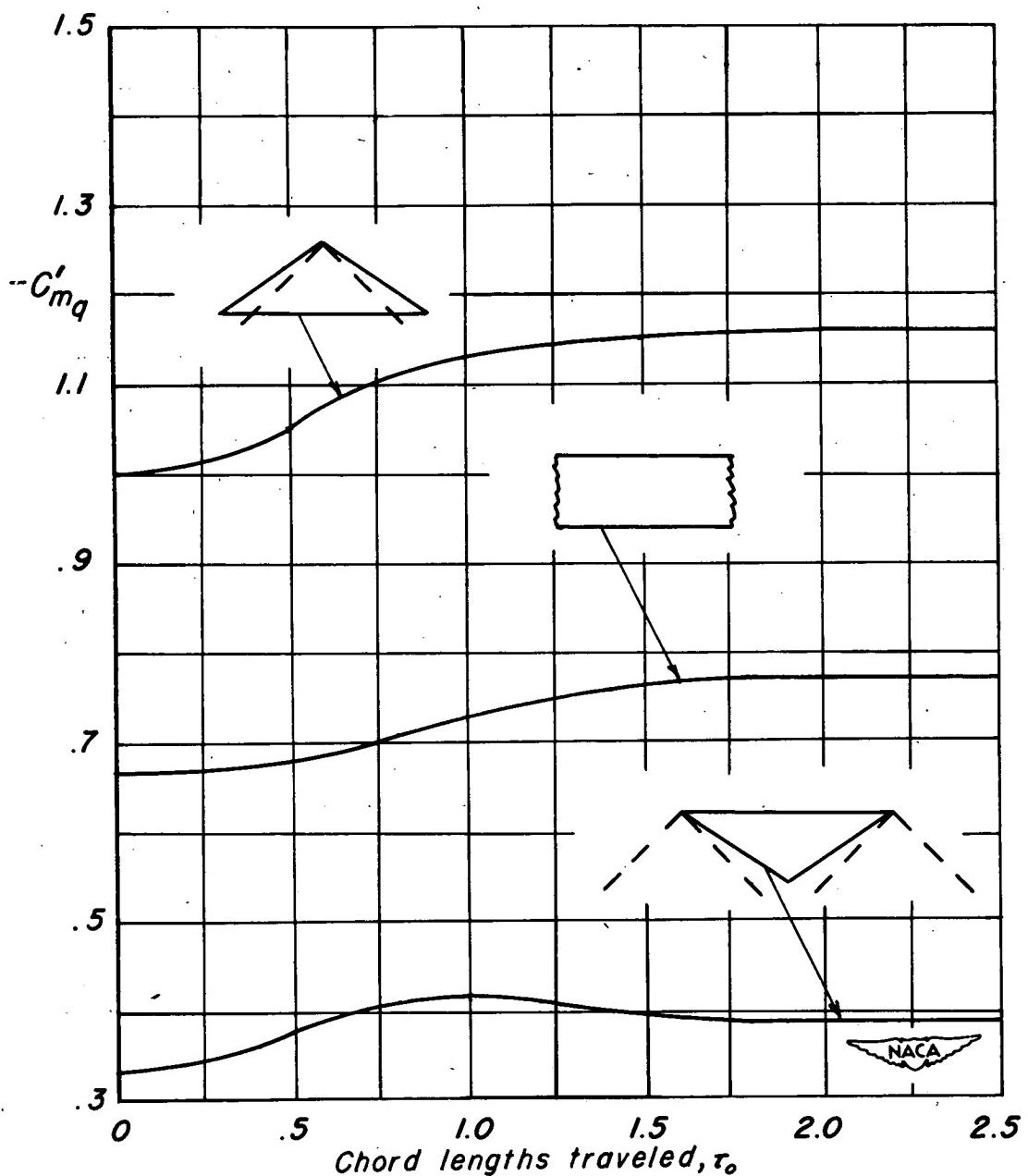
(b) Pitching moment about
    leading edge or apex.

Figure 5.- Continued.
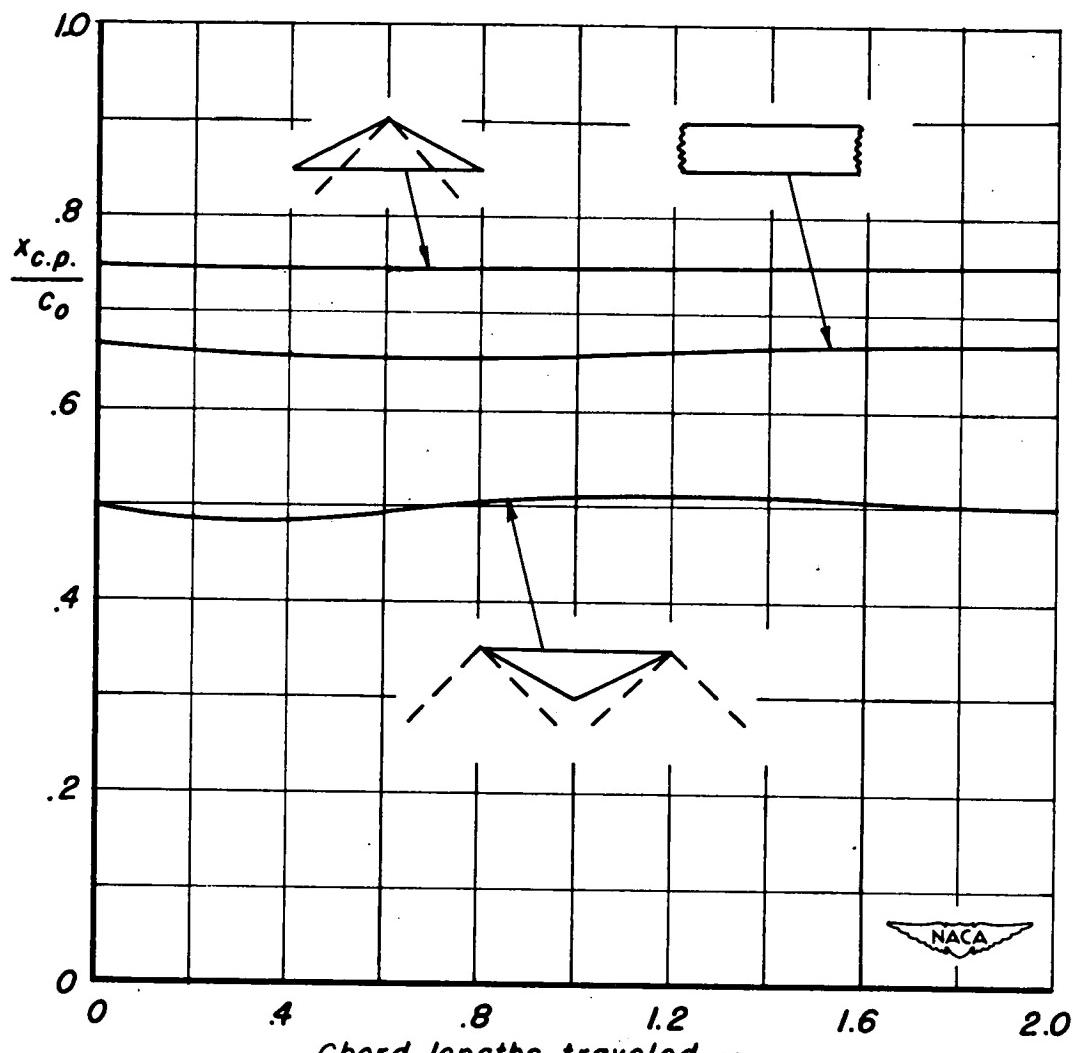
(c) Location of center of pressure
with reference to the leading
edge   or   apex.

Figure 5.— Concluded.
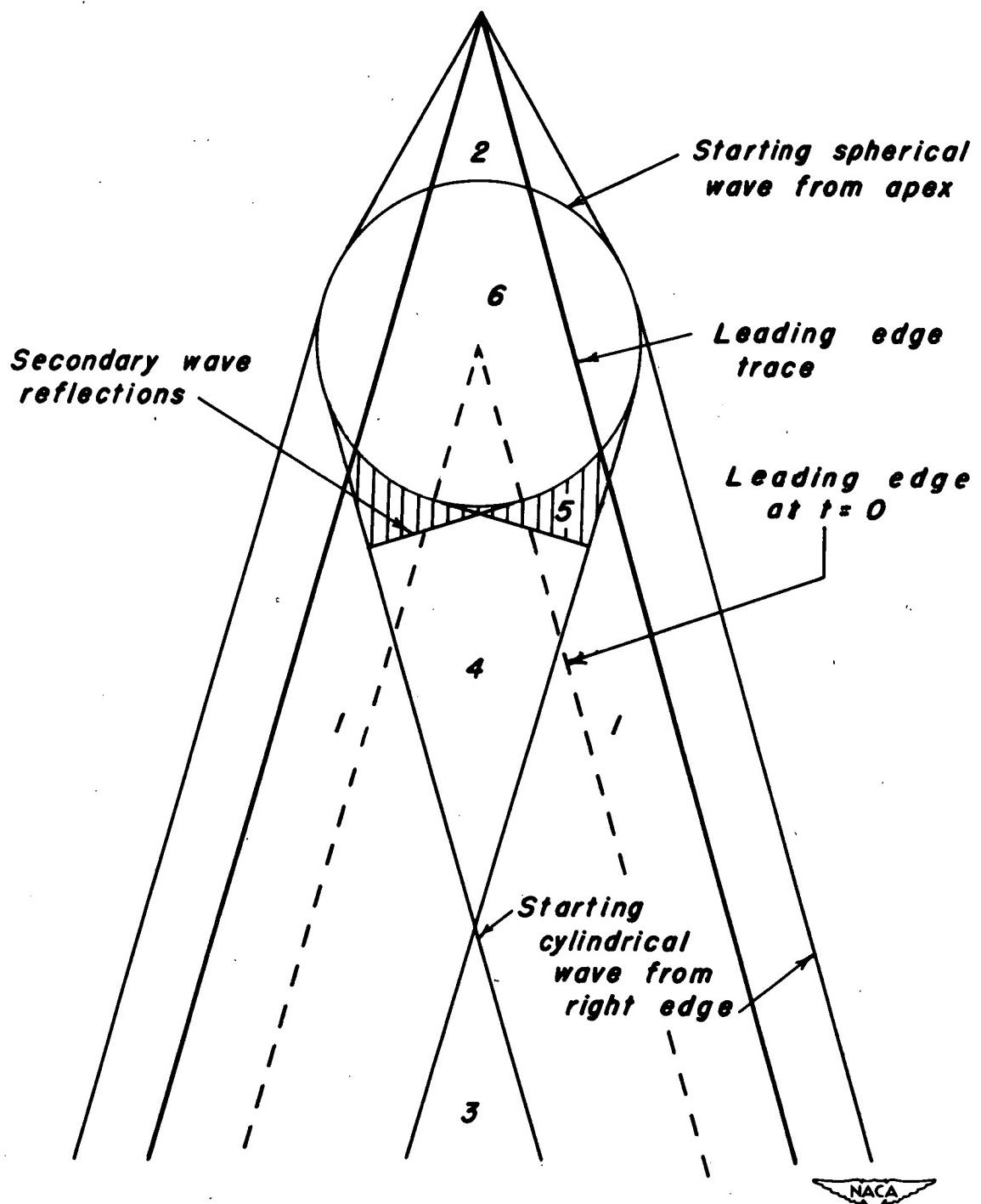
*Figure 6.— The six regions used in the analysis of the triangular wing with subsonic leading edges.*

$y = -(x + M_0 t)/\beta$

$y = -m(x + M_0 t)$

$m = ctn\Delta$

$\beta = \sqrt{M_0^2 - 1}$

$y = (x + M_0 t)/\beta$

$y = m(x + M_0 t)$

$y^2 + x^2 = t^2$

$M_0 t$

y

$y = mx + t\sqrt{1 + m^2}$

$y = -mx + t\sqrt{1 + m^2}$

$y = -mx - t\sqrt{1 + m^2}$

$y = mx - t\sqrt{1 + m^2}$

x
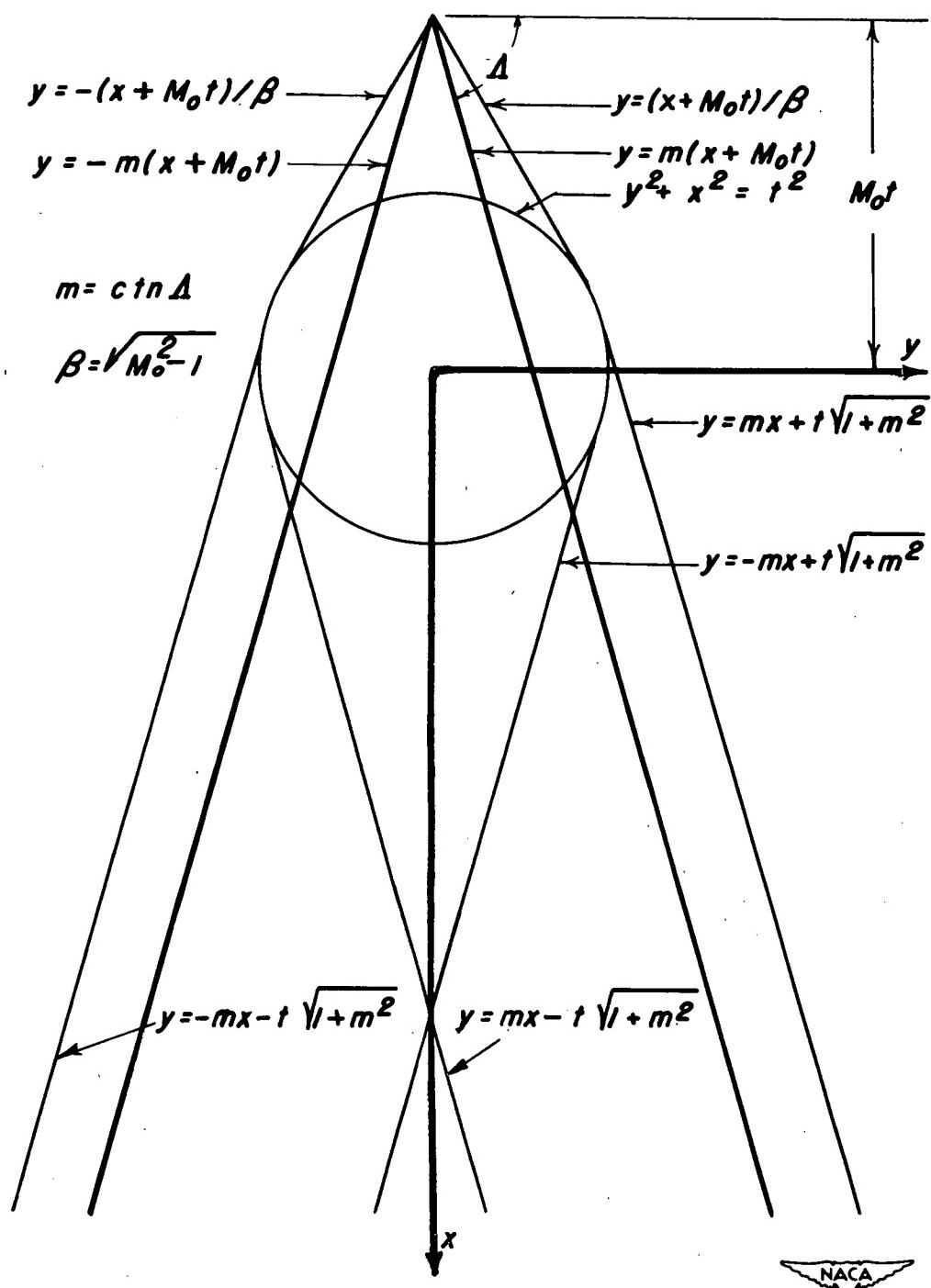
Figure 7.— Equations of lines pertinent to the analysis of the triangular wing with subsonic leading edges.
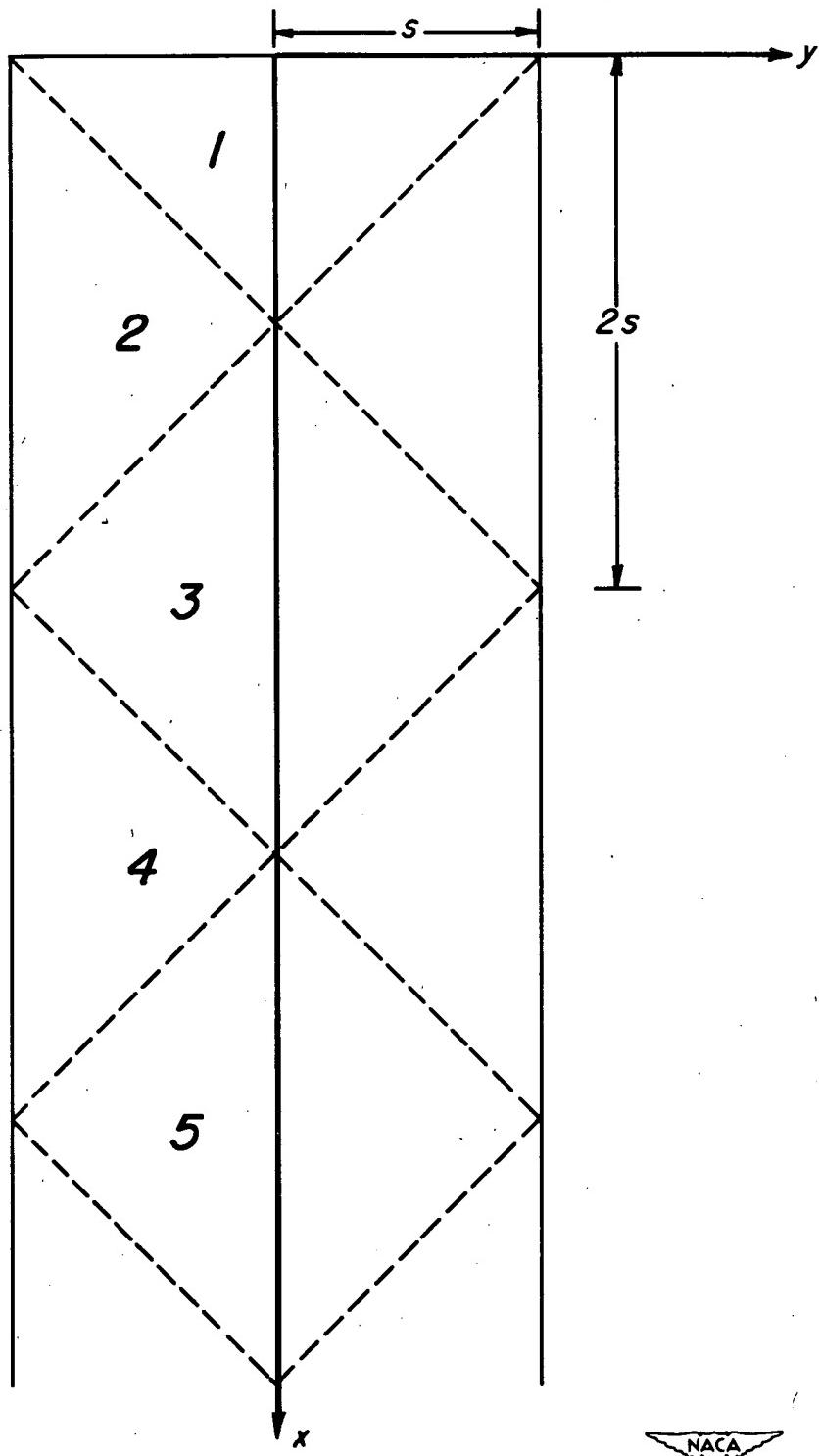
Figure 8.- Regions used in the discussion of the low-
aspect-ratio rectangular wing.

(a) Lift.

(b) Pitching moment about apex.
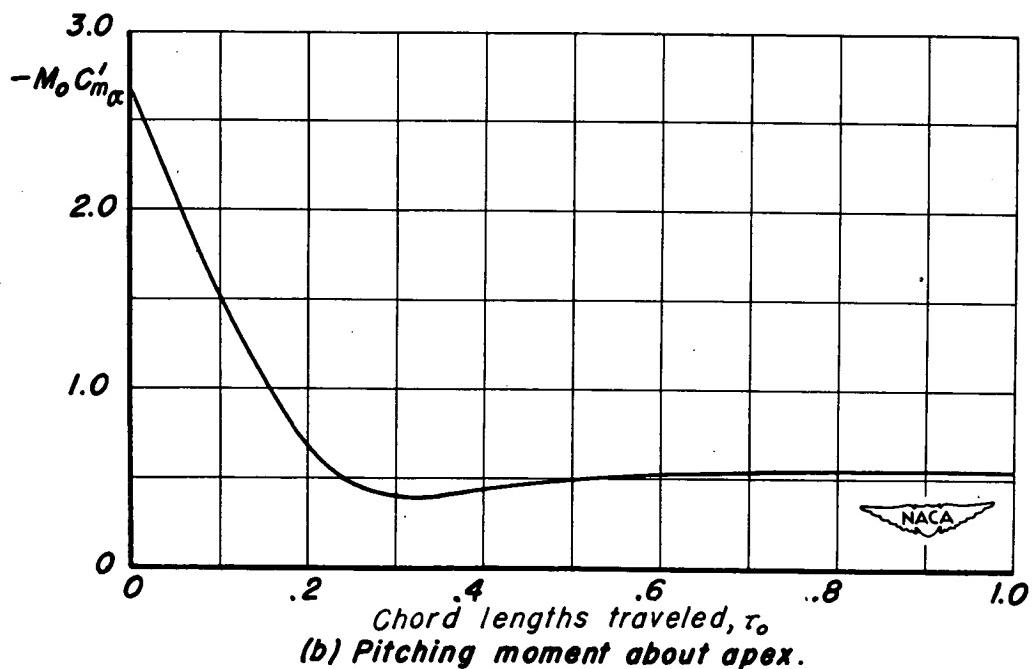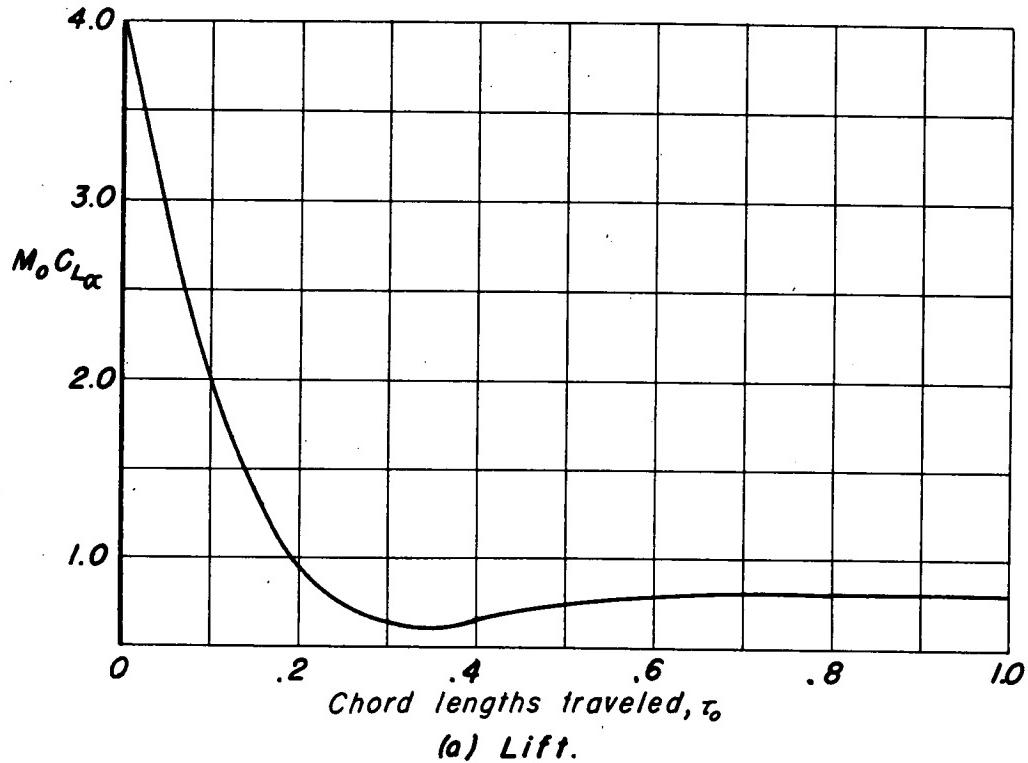
Figure 9.— Indicial aerodynamic characteristics of sinking triangular wings with slender plan forms. $mM_o = 1/8$.
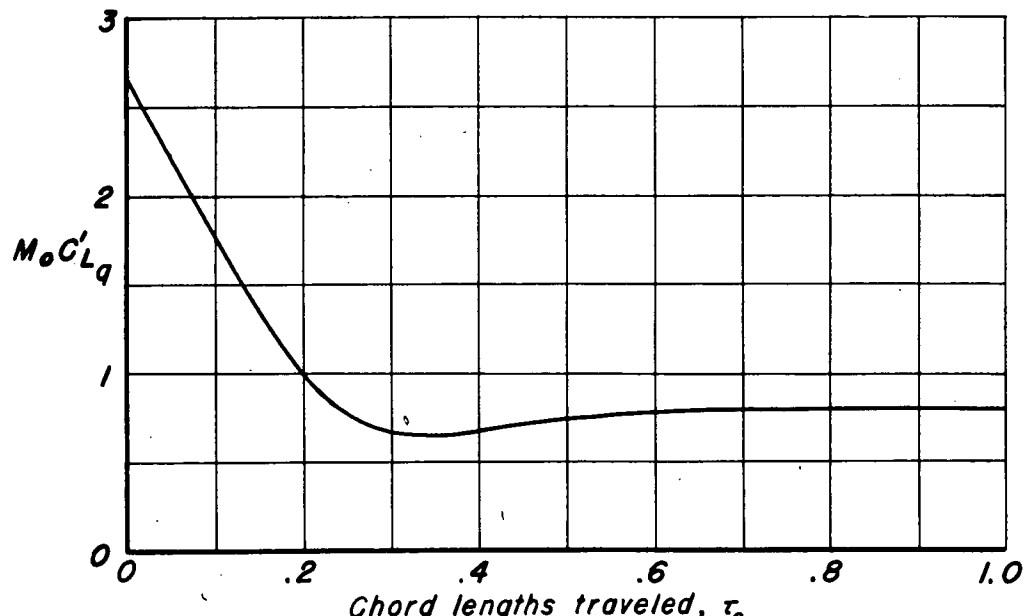
(a) Lift.
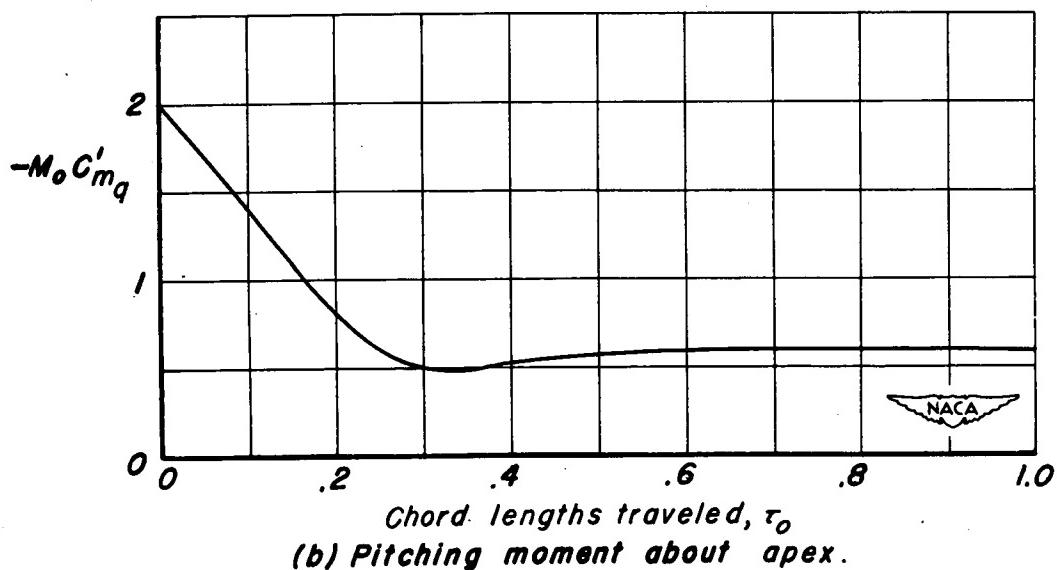
(b) Pitching moment about apex.

Figure 10.– Indicial aerodynamic characteristics of tri-
angular wings with slender plan forms pitching about
apex. $mM_0 = 1/8$.